

1 **Characterization and genomic analysis of the Lyme disease spirochete  
2 bacteriophage  $\phi$ BB-1**

3 Dominick R. Faith<sup>1\*</sup>, Margie Kinnersley<sup>1\*</sup>, Diane M. Brooks<sup>1</sup>, Dan Drecktrah<sup>1</sup>, Laura S.  
4 Hall<sup>1</sup>, Eric Luo<sup>2</sup>, Andrew Santiago-Frangos<sup>3</sup>, Jenny Wachter<sup>2</sup>, D. Scott Samuels<sup>1</sup>, and  
5 Patrick R. Secor<sup>1#</sup>

6 <sup>1</sup> Division of Biological Sciences, University of Montana, Missoula, MT, USA

7 <sup>2</sup> Vaccine and Infectious Disease Organization, Saskatoon, SK, Canada

8 <sup>3</sup> Department of Biology, University of Pennsylvania, Philadelphia, PA, USA

9 \*These authors contributed equally to this work

10 # Correspondence: [Patrick.secor@mso.umt.edu](mailto:Patrick.secor@mso.umt.edu)

11

12 **Abstract**

13 Lyme disease is a tick-borne infection caused by the spirochete *Borrelia*  
14 (*Borrelia*) *burgdorferi*. *Borrelia* species have highly fragmented genomes composed of  
15 a linear chromosome and a constellation of linear and circular plasmids that encode  
16 diverse outer membrane lipoproteins, which facilitate movement of the spirochete  
17 between its tick vector and a vertebrate host in an enzootic cycle. The *B. burgdorferi*  
18 genome shows evidence of horizontal transfer between strains, but the mechanisms  
19 remain poorly defined. Almost all Lyme disease spirochetes are infected by 32-kp circular  
20 plasmid (cp32) prophages that undergo lytic replication and produce infectious virions  
21 called  $\phi$ BB-1. In the laboratory,  $\phi$ BB-1 transduces cp32s and shuttle vectors between  
22 spirochetes. However, the extent that  $\phi$ BB-1 participates in horizontal gene transfer  
23 between Lyme disease spirochetes is not known. Here, we use proteomics and long-read  
24 sequencing to characterize  $\phi$ BB-1 virions and the genetic material they package. Our  
25 studies reveal that  $\phi$ BB-1 packages linear cp32s via a headful mechanism. We identify  
26 the cp32 *pac* region and show that plasmids containing the cp32 *pac* region are  
27 preferentially packaged into  $\phi$ BB-1 virions. Additionally, we find  $\phi$ BB-1 packages  
28 fragments of the linear chromosome and other plasmids including lp54, cp26, and others.  
29 Furthermore, sequencing of  $\phi$ BB-1 packaged DNA allowed us to resolve the covalently  
30 closed hairpin telomeres for the linear *B. burgdorferi* chromosome and most linear  
31 plasmids in strain CA-11.2A. Collectively, our results shed light on the biology of the  
32 ubiquitous  $\phi$ BB-1 phage and further implicates  $\phi$ BB-1 in the generalized transduction of  
33 diverse genes between spirochetes and the maintenance of genetic diversity in Lyme  
34 disease spirochetes.

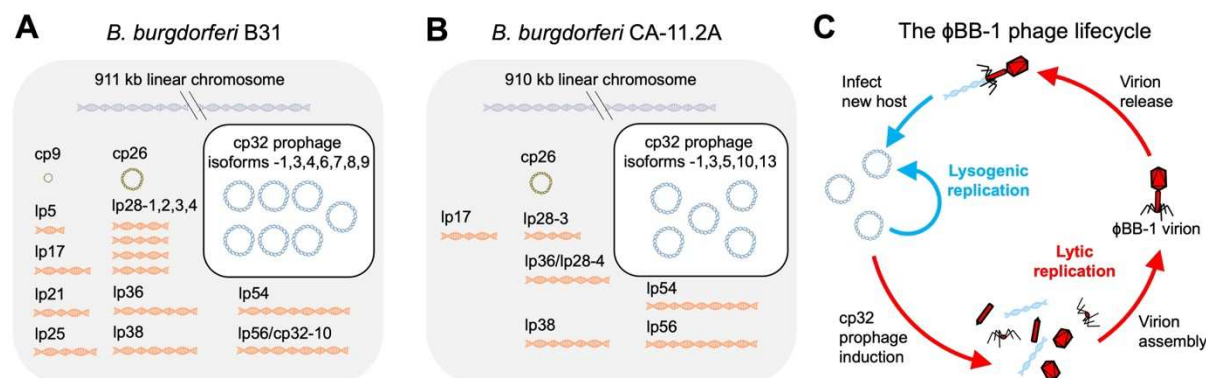
## 35 Introduction

36 The bacterium *Borrelia (Borrelia) burgdorferi* is the causative agent of Lyme  
37 disease, the most common tick-borne disease in the Northern Hemisphere [1-3]. Lyme  
38 disease spirochetes have complex and highly fragmented genomes composed of a ~900  
39 kb linear chromosome and a constellation of linear and circular plasmids that are similar  
40 but not identical across the genospecies [4-6].

41 A key factor in the ability of *B. burgdorferi* to transmit from its tick vector to a  
42 vertebrate host is the differential expression of several outer membrane lipoproteins that  
43 assist *B. burgdorferi* in evading both vector and host immune responses [7]. As such, a  
44 large fraction of the *B. burgdorferi* genome encodes outer membrane lipoproteins, mostly  
45 carried on the plasmids [6, 8, 9].

46 In natural populations, the recombination rate between genomes of coexisting *B.*  
47 *burgdorferi* strains exceeds the mutation rate and genetic variation in outer membrane  
48 lipoprotein alleles associated with species-level adaptations [6, 8-10]. Variation in outer  
49 membrane lipoprotein alleles across the genospecies is driven primarily by horizontal  
50 gene transfer [5, 11-17]. However, the mechanism(s) by which heterologous *B.*  
51 *burgdorferi* strains exchange genetic material are not well defined.

52 Viruses that infect bacteria (phages) are key drivers of horizontal gene transfer  
53 between bacteria [18]. The genomes of nearly all Lyme disease spirochetes include the  
54 32-kb circular plasmid (cp32) prophages (**Fig 1A and B**) [4]. The cp32s carry several  
55 outer membrane lipoprotein gene families including *bdr*, *mlp*, and *ospE/ospF/elp* (erps),  
56 which are all involved in immune evasion [19-23] and exhibit sequence variation that is  
57 consistent with historical recombination amongst cp32 isoforms [24-26]. Recent work  
58 indicates that cp32 prophages are induced in the tick midgut during a bloodmeal [9, 27,  
59 28]. When induced, cp32 prophages undergo lytic replication where they are packaged  
60 into infectious virions designated φBB-1 (**Fig 1C**) [29-31].



61  
62 **Figure 1. The *B. burgdorferi* genome is highly fragmented and is composed of a linear chromosome,**  
63 **linear and circular plasmids, and cp32 prophages.** The genomes of *B. burgdorferi* strains (**A**) B31 and  
64 (**B**) CA-11.2A are shown. (**C**) The temperate φBB-1 phage lifecycle is depicted.

65 In addition to horizontally transferring phage genomes between bacterial hosts  
66 (transduction), phages frequently package and horizontally transfer pieces of the bacterial  
67 chromosome or other non-phage DNA (generalized transduction) [32]. Generalized

68 transduction was first observed in the *Salmonella* phage P22 in the 1950s [33]. Since  
69 then, generalized transduction has been observed in numerous other phage species [32,  
70 34-37].  $\phi$ BB-1 is a generalized transducing phage that can horizontally transfer shuttle  
71 vectors carrying antibiotic resistance cassettes between *B. burgdorferi* strains [29].  
72 However, to our knowledge, generalized transduction of anything other than engineered  
73 plasmids by  $\phi$ BB-1 has not been observed.

74 Here, we define the genetic material packaged by  $\phi$ BB-1 virions isolated from *B.*  
75 *burgdorferi* strain CA-11.2A. Our proteomics studies confirm that  $\phi$ BB-1 virions are  
76 composed primarily of capsid and other phage structural proteins encoded by the cp32s;  
77 however, putative phage structural proteins encoded by lp54 were also detected. Long-  
78 read sequencing reveals that  $\phi$ BB-1 virions package a variety of genetic material  
79 including cp32 isoforms that are linearized at a region immediately upstream of the *erp*  
80 locus (*ospE/ospF/elp*) and packaged into  $\phi$ BB-1 capsids via a headful genome packaging  
81 mechanism at a packaging site (*pac*). When introduced to a shuttle vector, the *pac* region  
82 promotes the packaging of shuttle vectors into  $\phi$ BB-1 virions, demonstrating the utility of  
83  $\phi$ BB-1 as a tool to genetically manipulate Lyme disease spirochetes. Additionally, full-  
84 length contigs of cp26, lp17, lp38, lp54, and lp56 are recovered from packaged reads as  
85 are fragments of the linear chromosome. Finally, long-read sequencing of packaged DNA  
86 allowed us to fully resolve most of the covalently closed hairpin telomeres in the *B.*  
87 *burgdorferi* CA-11.2A genome.

88 Overall, this study implicates  $\phi$ BB-1 in mobilizing large portions of the *B.*  
89 *burgdorferi* genome, which may explain certain aspects of genome stability and diversity  
90 observed in Lyme disease spirochetes.

## 91 **Results**

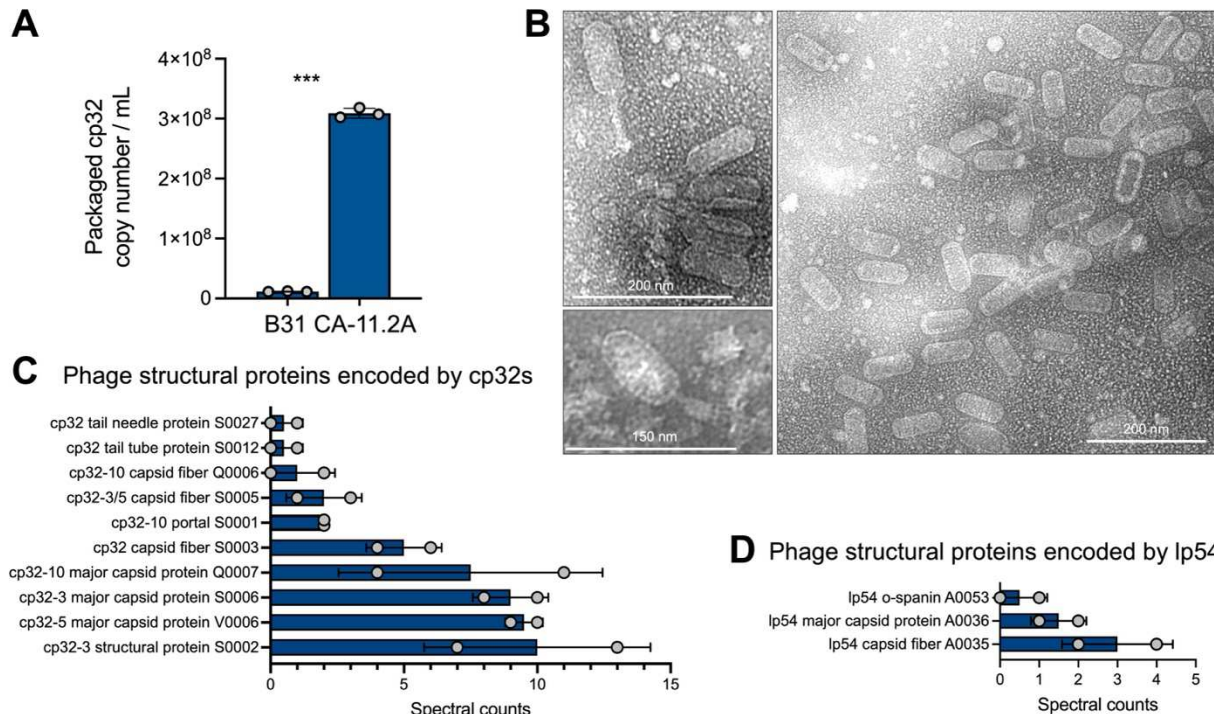
### 92 $\phi$ BB-1 phage purification, virion morphology, and proteomic analysis

93 In the laboratory, lytic  $\phi$ BB-1 replication (**Fig 1C**) can be induced by fermentation  
94 products such as ethanol [38, 39]. We first measured  $\phi$ BB-1 titers in early stationary-  
95 phase cultures ( $\sim 1 \times 10^8$  cells/mL) of *B. burgdorferi* B31 or CA-11.2A induced with 5%  
96 ethanol, as described by Eggers *et al.* [38]. Seventy-two hours after induction, bacteria  
97 were removed by centrifugation and filtering and virions were purified from supernatants  
98 by chloroform extraction and precipitation with ammonium sulfate. Purified virions were  
99 treated overnight with DNase to destroy DNA not protected within a capsid. Phage DNA  
100 was then extracted using a proteinase K/SDS/phenol-chloroform DNA extraction protocol  
101 and qPCR was used to measure packaged cp32 copy numbers.

102 *B. burgdorferi* strain CA-11.2A consistently produced  $\sim 10$  times more phage than  
103 B31 (**Fig 2A**) and was selected for further study. Imaging of purified virions collected from  
104 CA-11.2A by transmission electron microscopy reveals virions with an elongated capsid  
105 and contractile tail (**Fig 2B**), which is similar to the Myoviridae morphology of  $\phi$ BB-1  
106 virions produced by strain B31 *in vitro* [9, 40, 41] and by a human *B. burgdorferi* isolate  
107 following ciprofloxacin treatment [42].

108 Mass spectrometry analysis of purified virions identified ten capsid and other

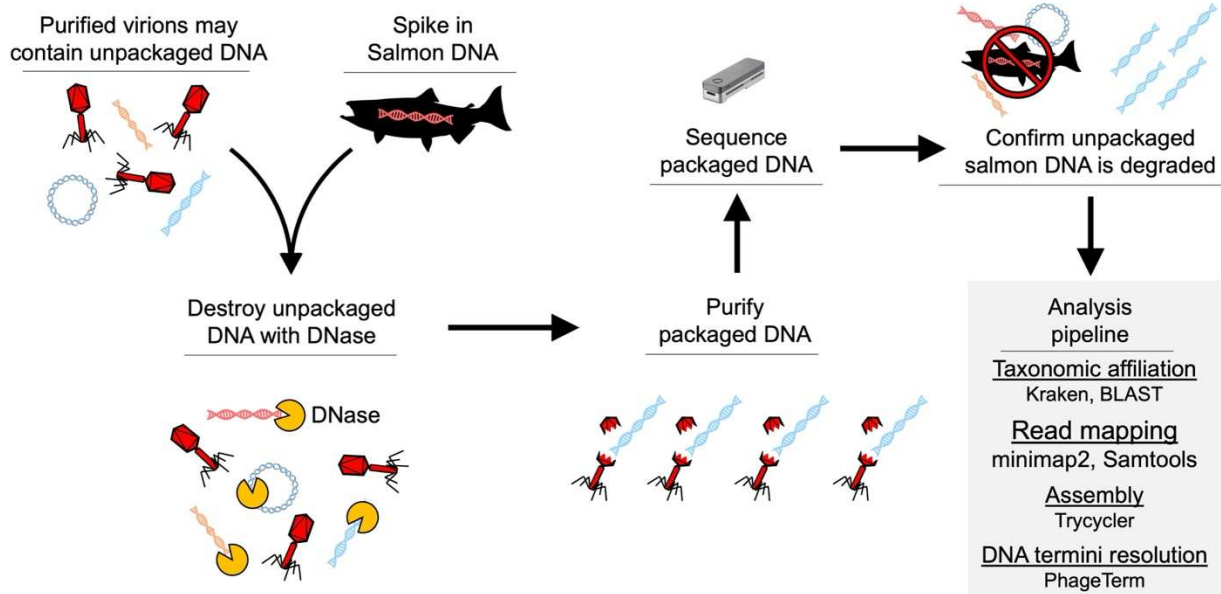
109 structural proteins encoded by the cp32s (**Fig 2C, Table S1**). We also detected highly  
110 conserved predicted phage capsid proteins encoded by lp54 (**Fig 2D**). While the virions  
111 we visualized all appear to have the same elongated capsid morphology, virions with a  
112 notably smaller capsid morphology have been isolated and imaged from *B. burgdorferi*  
113 CA-11.2A [29]. These observations raise the possibility that there are multiple intact  
114 phages inhabiting the CA-11.2A genome.



115  
116 **Figure 2.  $\phi$ BB-1 phage titer, virion morphology, and proteomic analysis.** (A) Packaged, DNase-  
117 protected cp32 copy numbers in bacterial supernatants were measured by qPCR. Data are the SE of the  
118 mean of three experiments, \*\*\*P<0.001. (B) Virions were purified from 4-L cultures of *B. burgdorferi* CA-  
119 11.2A and imaged by transmission electron microscopy. Representative images from two independent  
120 preparations are shown. (C and D) HPLC-MS/MS-based proteomics was used to identify proteins in the  
121 two purified virion preparations. The SE of the mean of spectral counts for peptides associated with the  
122 indicated phage structural proteins are shown for each replicate. See also **Table S1** for the complete  
123 proteomics dataset.

#### 124 $\phi$ BB-1 virions package portions of the *B. burgdorferi* genome

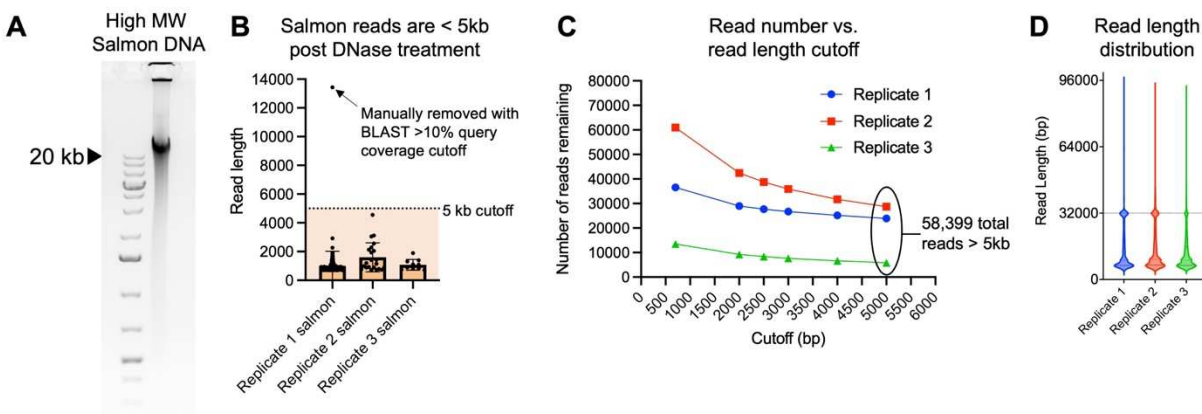
125 We performed long-read sequencing on DNA packaged in purified  $\phi$ BB-1 virions,  
126 as outlined in **Figure 3**. There is concern that contaminating unpackaged *B. burgdorferi*  
127 chromosomal or plasmid DNA co-purifies with phage virions. To control for this, we spiked  
128 purified  $\phi$ BB-1 virions with high molecular weight (> 20 kb) salmon sperm DNA (**Fig 4A**)  
129 at 1.7  $\mu$ g/mL, a concentration that approximates the amount of DNA released by  $3 \times 10^8$   
130 lysed bacterial cells into one milliliter of media [43]. Samples were then treated with  
131 DNase overnight followed by phage DNA extraction using a proteinase K/SDS/phenol-  
132 chloroform DNA extraction protocol [30]. Recovered DNA was directly sequenced using  
133 the Nanopore MinION (long read) platform.



134

135 **Figure 3. Workflow for sequencing packaged  $\phi$ BB-1 DNA.**

136 Kraken [44] was used to classify prokaryotic and eukaryote sequences followed by  
 137 BLAST to classify reads missed by Kraken (e-value <0.01, query coverage >10%). Reads  
 138 less than 700 bp were discarded. Of 110,986 reads >700 bp, 0.14% were classified as  
 139 matching salmon sequences (Fig 4B) with an average length of 1.2 kb (Fig 4B), indicating  
 140 the DNase treatment step successfully degraded unpackaged DNA. To exclude reads  
 141 that may be derived from unpackaged DNA, we removed all reads less than 5 kb from  
 142 the dataset, leaving a total of 58,399 reads longer than 5 kb (Fig 4C) with a median length  
 143 of 12.3 kb (Fig 4D). Note that cp32 prophages are approximately 32 kb in size and we  
 144 detect a high number of ~32 kb reads in each replicate (Fig 4D, dashed line).



145

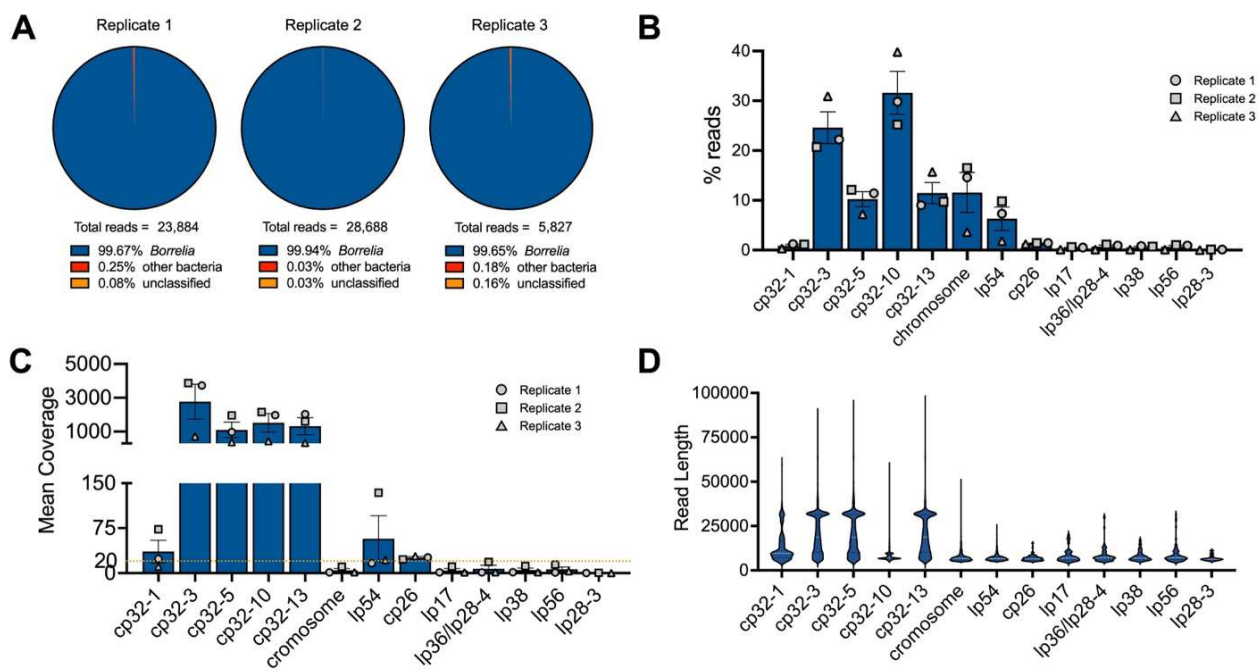
146 **Figure 4. Establishing a 5kb read length cutoff to exclude unpackaged reads.** (A) The salmon sperm  
 147 DNA used to spike purified phages prior to DNase treatment was run on an agarose gel to estimate its size.  
 148 Note that the majority of salmon DNA is larger than the 20-kb high molecular weight marker in the left lane.  
 149 (B) 0.14% of 110,986 reads > 700 bp, 0.14% were classified as matching salmon sequences. Reads  
 150 classified as salmon were plotted as a function of their length for each replicate. Error bars represent the  
 151 SE of the mean of three replicate experiments. All reads except one (arrow) were below 5 kb in length  
 152 (dashed line) with an average length of 1.2 kb. (C) Read length cutoff was plotted as a function of the  
 153 number of reads remaining in each replicate dataset. In total, 58,399 reads remain after establishing a 5-  
 154 kb cutoff. (D) Read length for all reads >5 kb in each replicate was plotted.

155 Overall, ~99.6% of packaged reads >5 kb were classified as *B. burgdorferi* (**Fig**  
156 **5A**), the majority of which (~79%) were cp32 isoforms (**Fig 5B**). Cp32-10 and cp32-3  
157 were preferentially packaged (~32% and ~25%, respectively) followed by cp32-13 and  
158 cp32-5 (each at ~10%) (**Fig 5B**). Reads mapping to cp32-3, cp32-5, cp32-10, and cp32-  
159 13 had a mean coverage of over 1,000× (**Fig 5C**). Cp32-1 reads accounted for only about  
160 one percent of all packaged reads (**Fig 5B**) and had lower mean coverage of  
161 approximately 36× (**Fig 5C**), suggesting that cp32-1 was not undergoing lytic replication.  
162 Read length distributions for the cp32s indicate that full-length ~32 kb molecules were  
163 frequently recovered for each cp32 isoform, except for cp32-10 (**Fig 5D**).

164 Additionally, 11.6% of reads > 5 kb mapped to the linear chromosome and ~6.3%  
165 of reads >5 kb mapped to lp54 (**Fig 5B**). The remaining reads mapped to *B. burgdorferi*  
166 plasmids cp26, lp17, lp36/lp28-4, lp38, lp56, and lp28-3 at 1–2% each (**Fig 5B**). *De novo*  
167 assembly of packaged reads produced full-length contigs of all cp32s, lp17, cp26, lp36,  
168 lp38, lp54, and lp56 (**Fig S1**), suggesting that full-length versions of these plasmids are  
169 packaged by φBB-1.

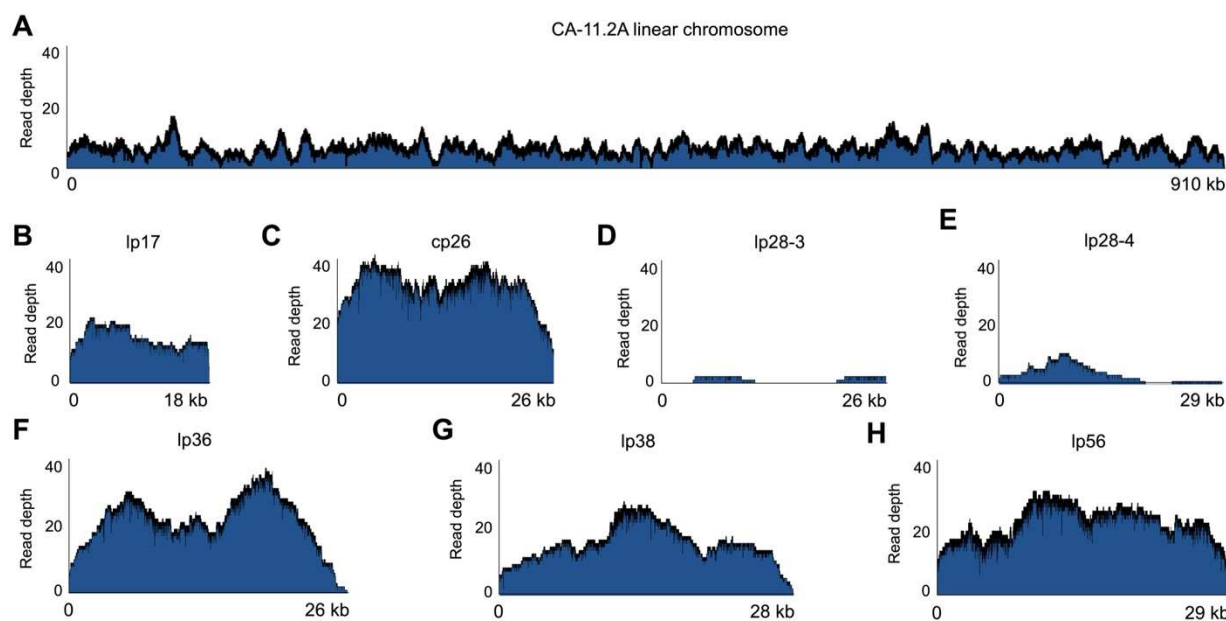
170 Of note, the CA-11.2A genome was reported to contain a unique plasmid,  
171 lp36/lp28-4, that is thought to have arisen from the fusion of lp36 with lp28-4 [45]. *De*  
172 *novo* assembly of packaged reads resolved lp36/lp28-4 into individual lp36 and lp28-4  
173 contigs (**Fig S1E and F**). Additionally, whole genome sequencing of our CA-11.2A strain  
174 confirmed that lp36 and lp28-4 are separate as no reads that span the lp36-lp28-4 junction  
175 were observed and coverage depth was notably different between lp36 and lp28-4 (~200×  
176 vs. 25×, respectively, **Fig S2A**). Furthermore, PCR confirmed the sequencing results (**Fig**  
177 **S2B-D**). These data indicate that the lp36/lp28-4 plasmid is two distinct episomes in our  
178 CA-11.2A strain.

179 Collectively, these results indicate that in addition to cp32 molecules, φBB-1 is  
180 capable of packaging non-cp32 portions of the *B. burgdorferi* genome. We discuss the  
181 major packaged DNA species in the following sections.



182

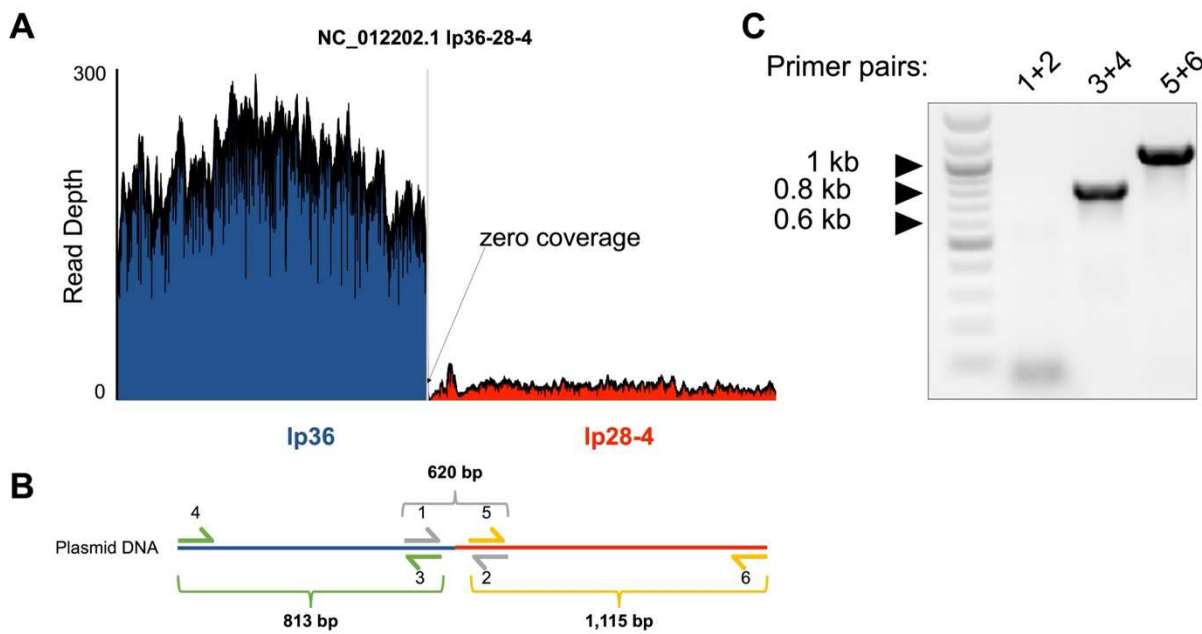
183 **Figure 5.  $\phi$ BB-1 virions package cp32 isoforms, chromosome fragments, lp54, and other plasmids.**  
184 **(A)** Kraken and BLAST were used to determine the taxonomic affiliation of reads >5kb. Note that no  
185 eukaryotic reads were identified. **(B and C)** The (B) percent and (C) mean coverage for reads affiliated with  
186 the indicated *B. burgdorferi* plasmid or linear chromosome are shown for each replicate. Error bars  
187 represent the SE of the mean. **(D)** Read length distributions for the indicated plasmids or chromosome are  
188 shown.



189

190 **Figure S1. Packaged read depth across the de novo CA-11.2A genome assembly.** De novo assembly  
191 of packaged reads >5kb produced the indicated contigs. Read coverage was then mapped to each contig.  
192 **(A-H)** Read coverage across the CA-11.2A chromosome or indicated plasmids are shown. Coverage maps  
193 for the cp32s and lp54 are shown in Figures 6 and 9, respectively.

194

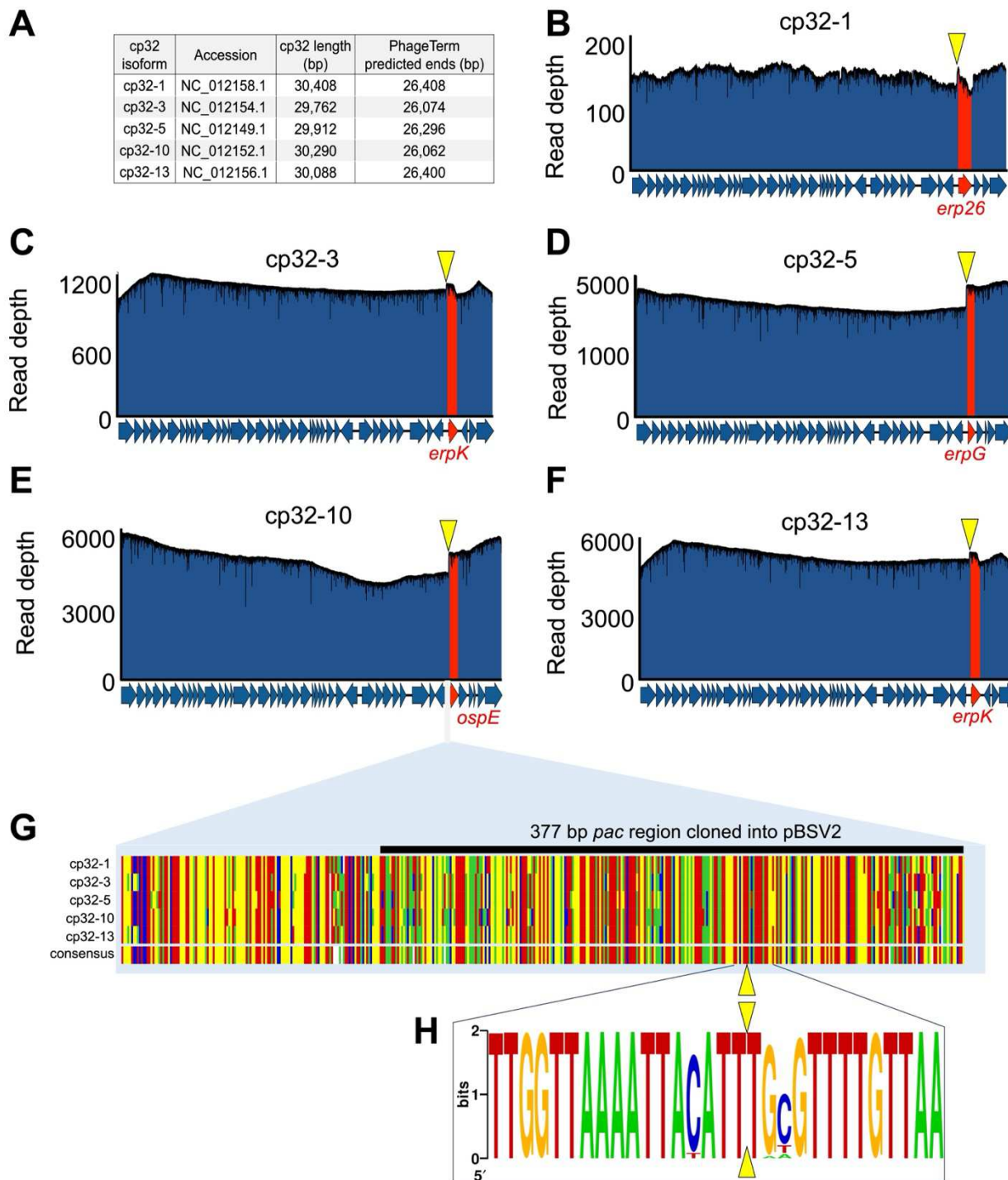


195

**Figure S2. Whole genome sequencing of the CA-11.2A genome reveals that plasmid Ip36/Ip28-4 resolves into two separate episomes.** (A) The CA-11.2A genome was sequenced using long-read technology. Reads were aligned to the Ip36/Ip28-4 reference sequence (NC\_012202.1) and read depth plotted. (B) Schematic of PCR design. Primers 1 and 2 flank the Ip36/Ip28-4 junction, with primer 1 annealing to Ip36 and primer 2 annealing to Ip28-4, creating a 620 bp product if joined. Primers 3 and 4 anneal to Ip36 DNA, creating an 813 bp product if present. Primers 5 and 6 anneal to Ip28-4 DNA, creating a 1,115 bp product if present. (C) The presence or absence of Ip36, Ip28-4, or Ip36/Ip28-4 was confirmed by PCR.

**204 cp32 molecules are linearized near the *erp* locus and packaged via a headful mechanism**

205 Our sequencing data provide insight into how  $\phi$ BB-1 packages cp32 molecules. 206 Many phage species package linear double-stranded DNA genomes that circularize after 207 being injected into a host [46] and packaged cp32s are thought to be linearized [30]. We 208 used PhageTerm [47] to predict the linear ends of packaged DNA. Native DNA termini 209 are present once per linear DNA molecule, but non-native DNA ends produced during 210 sequencing are distributed randomly along DNA molecules. Thus, reads that start at 211 native DNA terminal positions occur more frequently than anywhere else in the genome. 212 PhageTerm takes advantage of this to resolve DNA termini and predict phage packaging 213 mechanisms [47]. PhageTerm identified the termini of packaged cp32 molecules at 214 approximately 26 kb in a region lying immediately upstream of the *erp* (*ospE/ospF/elp*) 215 loci (**Fig 6A**). In agreement with the PhageTerm results, when packaged reads were used 216 to map the physical ends of packaged cp32 molecules, a sharp boundary in coverage 217 depth is observed upstream of the *ospE/ospF/elp* loci in all cp32s (**Fig 6B–F**). Notably, 218 the intergenic region upstream of the *erp* loci is conserved across the cp32 isoforms found 219 in diverse strains of Lyme disease spirochetes (**Fig 6G**) [15] and the linear cp32 ends 220 identified by long-read sequencing converge on the same terminal sequence motif (**Fig 221 6H**).



222

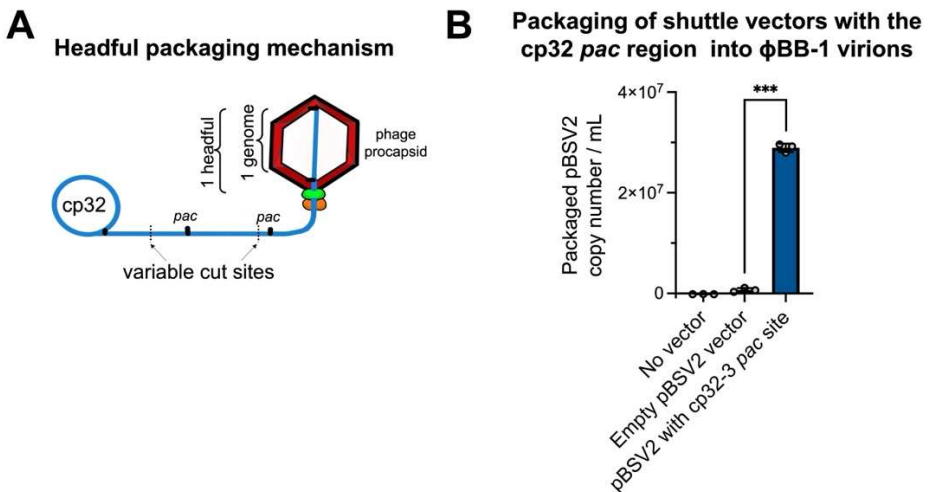
223 **Fig 6. cp32s are linearized upstream of the *erp* loci.** (A) PhageTerm was used to predict the linear ends  
 224 of packaged cp32 molecules. (B–F) Nanopore reads were mapped to the indicated cp32s. Note the sharp  
 225 boundary just upstream of the *erp* loci (highlighted in red). The yellow triangles indicate the PhageTerm  
 226 predicted linear ends. (G) Alignments of the intergenic region upstream of the *erp* loci is shown for each  
 227 cp32. The black line indicates the *pac* region that was cloned into a shuttle vector, as described in Figure  
 228 7. (H) A nucleic acid logo was constructed from 207 cp32 sequence alignments. Yellow triangles indicate  
 229 the linear end of cp32 isoforms as predicted by PhageTerm and confirmed by long-read sequencing.

230 PhageTerm predicts that cp32s are packaged by a headful mechanism. This  
 231 observation supports the previously proposed headful genome packaging mechanism for  
 232 cp32s [39]. Phages that use the headful packaging mechanism generate a concatemer

233 containing several head-to-tail copies of their genome (**Fig 7A**). During headful  
234 packaging, a cut is made at a defined packaging site (*pac* site) and a headful (a little more  
235 than a full genome) of linear phage DNA is packaged. Once a headful is achieved, the  
236 phage genome is cut at non-defined sites, resulting in variable cut positions and size  
237 variation in packaged DNA, which we observe in packaged cp32 reads downstream of  
238 the initial cut site (**Fig 6B–F**).

239 Our results suggest that the cp32 *pac* site is upstream of the *erp* (*ospE/ospF/elp*)  
240 loci. If the cp32 *pac* site is in this region, then DNA molecules containing the *pac* sequence  
241 are expected to be packaged into  $\phi$ BB-1 virions. To test this, we cloned the putative cp32-  
242 3 *pac* site (**Fig 6G**, black bar) into the pBSV2 shuttle vector [48], transformed *B.*  
243 *burgdorferi* strain CA-11.2A, and induced lytic  $\phi$ BB-1 replication with 5% ethanol.  
244 Supernatants containing virions were collected, filtered, and DNase treated, and  
245 packaged DNA isolated. pBSV2 shuttle vector copy numbers were measured by qPCR  
246 using primers that target the pBSV2 kanamycin resistance (*kan*) cassette. To control for  
247 possible chromosomal DNA contamination, qPCR was also performed using primers  
248 targeting the *flaB* gene. Final packaged pBSV2 copy numbers were calculated by  
249 subtracting *flaB* copy numbers from pBSV2 (*kan* cassette) copy numbers.

250 Copy numbers of packaged pBSV2 encoding the cp32-3 *pac* site were significantly  
251 ( $P<0.001$ ) higher compared to virions collected from cells either not carrying the pBSV2  
252 vector or cells carrying an empty pBSV2 vector (**Fig 7B**), indicating that DNA molecules  
253 that contain the *pac* site are preferentially packaged by  $\phi$ BB-1 virions.



254  
255 **Figure 7. Shuttle vectors containing the cp32 pac region are preferentially packaged into  $\phi$ BB-1**  
256 **virions.** (A) Schematic depicting the headful genome packaging mechanism. (B) After ethanol induction,  
257  $\phi$ BB-1 virions were collected from CA-11.2A cells not carrying plasmid pBSV2 (No vector), cells  
258 transformed with empty pBSV2, or cells transformed with pBSV2 with the cp32-3 pac site (see Fig 6G for  
259 the cloned pac region). Copy numbers of pBSV2 packaged into  $\phi$ BB-1 virions were measured by qPCR.  
260 Data are the SE of the mean of three experiments, \*\*\* $P<0.001$ .

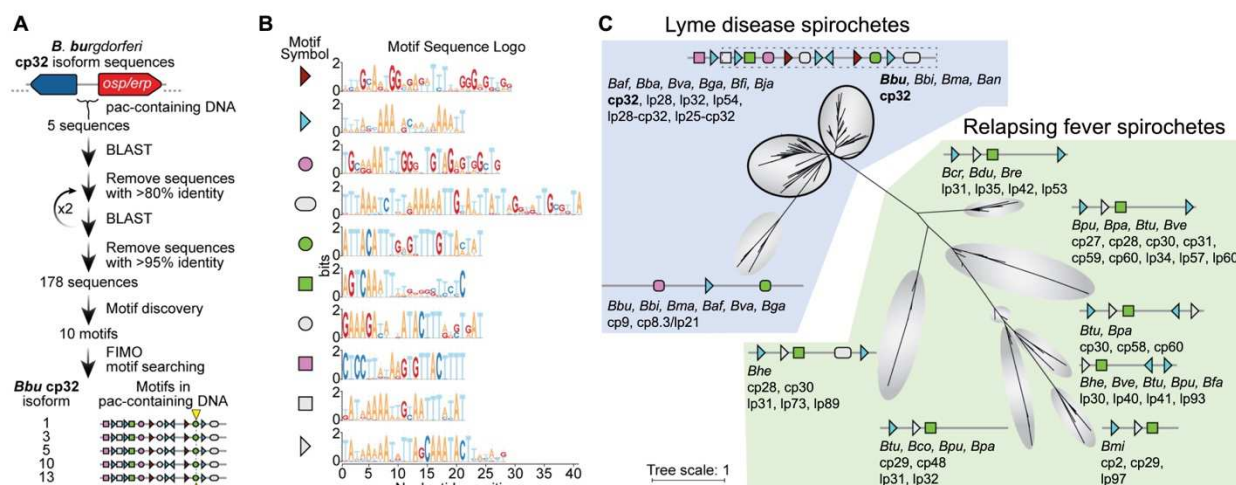
261 The cp32 prophages have conserved motifs that occur in a specific arrangement not  
262 found in other DNA sequences packaged by  $\phi$ BB-1 virions

263 To identify motif(s) that may be shared between the cp32s and other genomic

elements that are packaged into  $\phi$ BB-1 virions (e.g., lp54), we first used an iterative BLAST search to identify distantly homologous DNA sequences (Fig 8). A non-redundant list of these diverse DNA sequences were then used as an input dataset for sequence motif discovery via MEME [49]. All five cp32 isoforms found in *B. burgdorferi* CA-11.2A have the same specific arrangement of conserved sequence motifs around the pac region (Fig 8A and B) and these are conserved in cp32 isoforms across *B. burgdorferi* (Fig 8C). However, significant matches to these motifs were not identified in other CA-11.2A genetic elements packaged by  $\phi$ BB-1 (Supplementary Data file 1), suggesting that packaging of non-cp32 DNA may occur spontaneously or through different mechanisms.

273 The complete or partial arrangement of motifs found around the pac site of *B.*  
 274 *burgdorferi* cp32 isoforms is conserved in cp32 plasmids and some linear plasmids  
 275 originating from several different *Borrelia* species (**Fig. 8C**). The iterative BLAST search  
 276 also revealed that a diverse set of circular and linear plasmids in a broader set of *Borrelia*  
 277 species share some of the motifs found in *B. burgdorferi* cp32 isoforms. In total, linear or  
 278 circular plasmid sequences from 21 different *Borrelia* species (both Lyme disease and  
 279 relapsing fever spirochetes) had homology to the *B. burgdorferi* cp32 pac-containing DNA  
 280 sequences (**Fig 8C**). The motifs that are found most broadly, e.g., blue triangle, and green  
 281 square, may represent binding sites for conserved host factors that are present in all  
 282 these *Borrelia* species whereas the other motifs may represent protein-binding sites or  
 283 regulatory sequences that are specific to given prophage or plasmids.

284



285

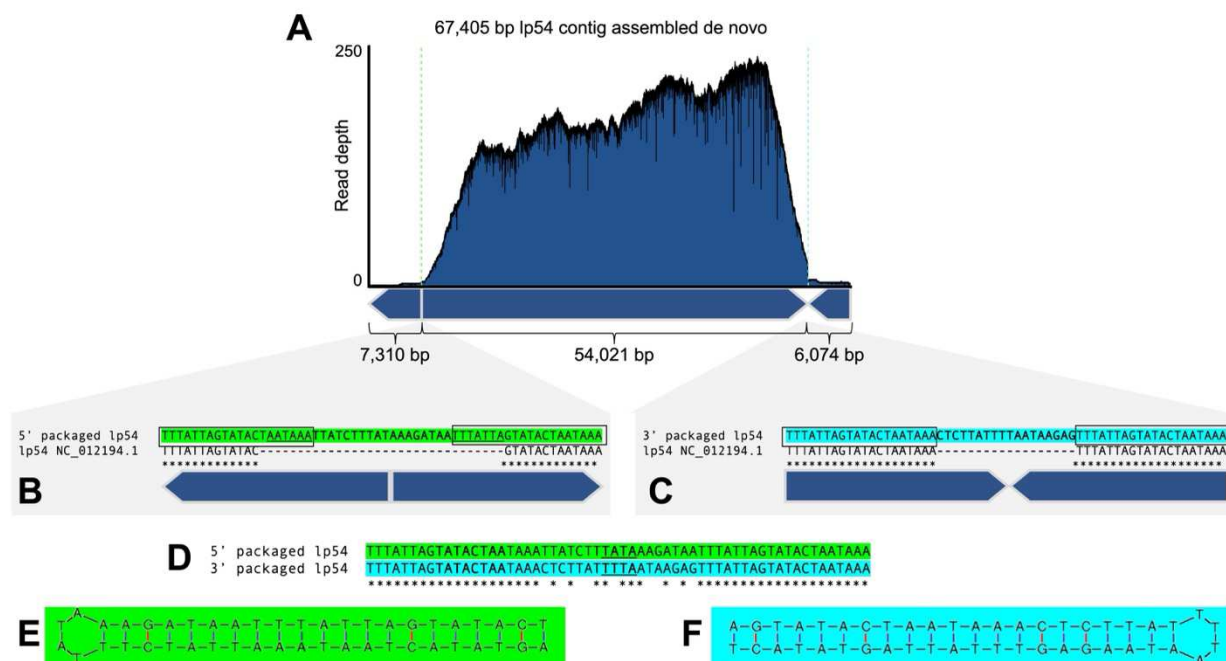
**Figure 8. Cp32 prophages have conserved motifs that occur in a specific arrangement around the pac site. (A)** Outline of bioinformatic strategy to identify motifs enriched in the pac-containing DNA sequence of cp32 isoforms. All *B. burgdorferi* cp32 isoforms have the same motifs in the pac region. The cp32 cut site is indicated by the yellow triangle. **(B)** Sequence logos of the motifs identified in panel A and schematized in panel C. Nine of the top ten motifs occur at least once in the pac-containing region of cp32 DNA sequences. Motifs represented with right or left facing triangles often occur as direct and/or indirect repeats. **(C)** Phylogenetic tree of non-redundant DNA sequences with homology to *B. burgdorferi* cp32 pac-region identified in panel A. For each clade, the bacterial species and type of plasmid are listed. For clarity in the figure, bacterial species names have been truncated to a three letter abbreviation consisting of the first letter of the genus and the first two letters of the species (*Borrelia afzelii*, *Baf*; *Borrelia andersonii*, *Ban*; *Borrelia bavariensis*, *Bba*; *Borrelia bissettiae*, *Bbi*; *Borrelia burgdorferi*, *Bbu*; *Borrelia coriaceae*, *Bco*; *Borrelia crocidurae*, *Bcr*; *Borrelia duttonii*, *Bdu*; *Borrelia fainii*, *Bfa*; *Borrelia finlandensis*, *Bfi*; *Borrelia garinii*,

298 *Bga*; *Borrelia hemsii*, *Bhe*; *Borrelia japonica*, *Bja*; *Borrelia mayonii*, *Bma*; *Borrelia miyamotoi*, *Bmi*; *Borrelia parkeri*, *Bpa*; *Borrelia puertoricensis*, *Bpu*; *Borrelia recurrentis*, *Bre*; *Borrelia turicatae*, *Btu*; *Borrelia valaisiana*, *Bva*; *Borrelia venezuelensis*, *Bve*). There is variability in the motif architecture between sequences within a single clade; however, for clarity, a representative motif architecture discovered by MEME is shown [49]. The top two clades of sequences (outlined in black) are dominated by cp32 isoforms and the cp32 motif architecture, therefore a single motif scheme is shown for these two clades. The region of DNA and motifs cloned into the pBSV2 shuttle vector is outlined in dashes.

305 **Deciphering the structure of linear plasmids packaged by  $\phi$ BB-1**

306 After the cp32s, lp54 is a major DNA species packaged by  $\phi$ BB-1 (Fig 5C). Lp54  
307 is a linear plasmid with covalently closed telomeric ends [50]. *De novo* assembly of  
308 packaged lp54 reads produces a 67.4 kb contig consisting of full-length lp54 (54,021 bp,  
309 NC\_012194.1) flanked by sequences containing tail-to-tail (7,310 bp) and head-to-head  
310 (6,074 bp) junctions (Fig 9A). Read depth for lp54 was >100 for most of the contig;  
311 however, read depth drops precipitously at both tail-to-tail and head-to-head junctions  
312 (Fig 9A), suggesting that the telomeres of lp54 interfere with sequencing.

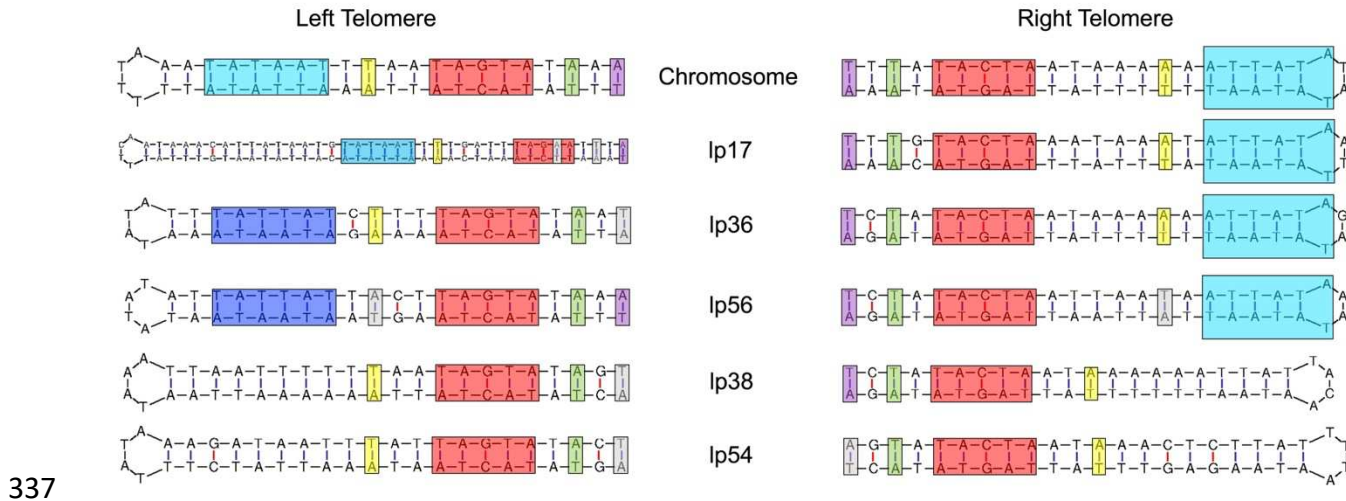
313 *B. burgdorferi* telomeres contain inverted repeat sequences [51] and we identified  
314 the CA-11.2A lp54 inverted repeat sequence as 5'-TTTATTAGTATACTAATAAAA (Fig 9B  
315 and C, boxed sequences). The 5' inverted repeat of the lp54 reference sequence is  
316 missing seven nucleotides and our data extends and completes this sequence (Fig 9B,  
317 underlined). Further, compared to the lp54 reference sequence, the packaged 5' and 3'  
318 junction-spanning sequences each encode an additional 18 bp of sequence (Fig 9B and  
319 C). These sequences, although unique at each end (Fig 9D), form perfect hairpin  
320 structures (Fig 9E and F). Overall, these data suggest that lp54 molecules with complete  
321 telomere sequences are packaged into virions. However, whether linear lp54 with  
322 covalently closed telomeres or lp54 replication intermediates that contain head-to-head  
323 and tail-to-tail junctions are packaged is unclear.



324  
325 **Figure 9. Full-length lp54 with fully resolved telomeres are recovered from  $\phi$ BB-1-packaged DNA.**  
326 (A) *De novo* assembly of packaged reads produced a 67,405 bp contig with tail-to-tail and head-to-head

327 junctions. **(B and C)** Sequences at the packaged 5' junction (green) or the 3' junction (cyan) are compared  
328 to the lp54 reference sequence NC\_012194.1. The conserved inverted repeat sequence 5'-  
329 TTTATTAGTATACTATAAAA is outlined. **(D)** Alignments of the tail-to-tail and head-to-head junctions  
330 reveals a variable 18-bp sequence in between the conserved inverted repeats. **(E and F)** Predicted hairpin  
331 structures are shown for each end of lp54. The loop sequence for each hairpin is underlined in panel D.

332 The *de novo* assembly approach applied to lp54 was also successful in resolving  
333 the telomeric ends of other linear elements of the CA-11.2A genome, including the linear  
334 chromosome and plasmids lp17, lp56, and lp38 (**Fig 10**). Additionally, we were able to  
335 resolve left and right telomeres for lp36 (**Fig 10**), providing yet further evidence that lp36  
336 is not fused to lp28-4.



338 **Figure 10. Packaged reads resolve the telomeric ends of the linear chromosome and most linear**  
339 **plasmids in the CA-11.2A genome.** Reads spanning tail-to-tail or head-to-head junctions of the linear  
340 **chromosome or the indicated linear plasmids form perfect hairpin structures. Conserved regulatory**  
341 **elements for each telomere are highlighted [52-57].**

342 **Discussion**

343 In nature, Lyme disease spirochetes exist as diverse populations of closely related  
344 bacteria that possess sufficient antigenic variability to allow them to co-infect and reinfect  
345 non-naïve vertebrate hosts [58-69]. Moreover, horizontal gene transfer between Lyme  
346 disease spirochetes has been extensively documented [70-75]. Nevertheless, the  
347 mechanism underlying horizontal genetic exchange among Lyme disease spirochetes  
348 remains undefined.

349 Horizontal gene transfer between heterologous spirochetes likely occurs in the tick  
350 midgut during and immediately after a blood meal when spirochete replication rates and  
351 densities are at their highest.  $\phi$ BB-1 replication is also induced in the tick midgut during a  
352 bloodmeal [9, 27, 28] and homologous recombination between cp32 isoforms [15-17] and  
353 the horizontal transfer of cp32s between *Borrelia* strains has been documented [25].  
354 These observations implicate  $\phi$ BB-1 in mediating horizontal gene transfer between Lyme  
355 disease spirochetes.

356 Our study further implicates  $\phi$ BB-1 in mediating horizontal gene transfer between  
357 Lyme disease spirochetes. Our sequencing data indicate that  $\phi$ BB-1 virions package  
358 portions of the entire *B. burgdorferi* genome, giving  $\phi$ BB-1 the potential to mobilize  
359 numerous beneficial alleles during the enzootic cycle via generalized transduction. For  
360 example, the circular cp32 prophages are highly conserved across the *Borrelia* genus  
361 [22]; however, cp32 isoforms contain variable regions that encode outer membrane  
362 lipoproteins such as Bdr, Mlp, and OspE/OspF/Elp, which are known to facilitate the *B.*  
363 *burgdorferi* lifecycle [20, 22, 23, 76]. The linear plasmid lp54 encodes the outer membrane  
364 lipoproteins OspA and OspB, which are required for *B. burgdorferi* to colonize the tick  
365 midgut [77-79]. The outer membrane lipoprotein OspC, which is required for *B.*  
366 *burgdorferi* to infect a vertebrate host, is encoded by the circular plasmid cp26 [58, 74,  
367 80]. All these alleles (and many others) are packaged by  $\phi$ BB-1, which is consistent with  
368 a role for phage-mediated transduction of genes encoding essential membrane  
369 lipoproteins between heterologous spirochetes.

370 In *B. burgdorferi*, the linear chromosome is highly conserved as are the circular  
371 plasmids cp32 and cp26 and the linear plasmids lp17, lp38, lp54, and lp56 are  
372 evolutionarily stable [4-6, 16, 81]. However, other plasmids distributed across the  
373 genospecies show considerably more variation and encode mostly (87%) pseudogenes  
374 and are thought to be in a state of evolutionary decay [6]. The plasmids we identified as  
375 packaged by  $\phi$ BB-1 virions include the cp32s, cp26, lp17, lp38, lp54, and lp56—the same  
376 plasmids that are evolutionarily stable across the genospecies [4-6, 16, 81]. These  
377 observations suggest that genes encoded on  $\phi$ BB-1-packaged plasmids are under  
378 positive selection, possibly as a result of transduction between Lyme disease spirochetes  
379 during the enzootic cycle.

380 In addition to providing evidence that  $\phi$ BB-1 virions package large portions of the  
381 *B. burgdorferi* genome, our study provides insight into  $\phi$ BB-1 virion structure and identifies  
382 virion proteins present in  $\phi$ BB-1. Using mass spectrometry-based proteomics, we confirm  
383 that putative capsid and other predicted structural genes encoded by cp32s such as the

384 major capsid protein P06 are indeed translated and assembled into mature  $\phi$ BB-1 virions.

385 Our long-read sequencing studies indicate that  $\phi$ BB-1 packages full-length linear  
386 cp32 molecules via a headful mechanism using *pac* sites. The headful packaging  
387 mechanism is used by numerous phages and was first described for *E. coli* phage T4 in  
388 1967 [82]. After injecting linear DNA into a new host, the phage genome re-circularizes  
389 before continuing its replication cycle. Genes encoded near the ends of linear phage  
390 genomes are subject to copy number variation and recombination as the phage genome  
391 re-circularizes [83]. Our data suggest that the conversion of linear cp32 molecules into  
392 circular cp32 molecules occurs in the vicinity of the *erp* locus, which could facilitate  
393 recombination with polymorphic *erp* alleles encoded by other cp32 isoforms in diverse *B.*  
394 *burgdorferi* hosts.

395 In this study, the packaging of specific cp32 isoforms was biased: cp32-3, cp32-5,  
396 cp32-10, and cp32-13 were predominantly packaged while cp32-1 was rarely packaged.  
397 This result is consistent with observations by Wachter *et al.* where cp32 isoform copy  
398 number and transcriptional activity were not uniform across all cp32 isoforms in *B.*  
399 *burgdorferi* strain B31: cp32-1, cp32-3, and cp32-6 were predominantly induced (highest  
400 copy numbers) and had the highest transcriptional activity while cp32-9 was not induced  
401 and was transcriptionally inactive [9]. Variability in the *pac* region or other regulatory  
402 elements involved in cp32 induction may explain why different cp32 isoforms replicate  
403 and/or are packaged at different rates.

404 In the intergenic region upstream of the *erp* loci, we identified a 377-bp region that  
405 contains the cp32 *pac* signal. Introducing the cp32 *pac* region to a shuttle vector facilitated  
406 the packaging of the shuttle vector into  $\phi$ BB-1 virions. Identification of the cp32 *pac* site  
407 will be useful for the engineering of recombinant DNA that can be packaged into virions  
408 that infect spirochetes, giving  $\phi$ BB-1 the potential for use as a genetic tool.

409 After the cp32s, lp54 was the most frequently packaged plasmid. This may be  
410 related to the evolutionary origins of lp54: lp54 contains large blocks of homology with the  
411 cp32s and is thought to have emerged from an ancient recombination event between a  
412 cp32 and a linear plasmid [6]. In addition, lp54 encodes putative phage proteins including  
413 a porin (BBA74) [84] and phage capsid proteins that are highly conserved across the  
414 genospecies [85], which we detected in purified virions by mass spectrometry. While we  
415 observed virions with a distinct elongated capsid morphology, virions with a notably  
416 smaller capsid morphology have been observed after induction *in vitro* [9, 29, 30]. These  
417 observations raise the possibility that lp54 may be a prophage, although whether lp54  
418 produces its own capsids or relies on cp32-encoded capsids, or if lp54 capsid proteins  
419 assemble with capsid proteins encoded by cp32 to produce chimeric capsids, is not clear.

420 Our long-read dataset contained reads that spanned head-to-head and tail-to-tail  
421 junctions in lp54. These reads allowed us to define the lp54 telomere sequences;  
422 however, whether full-length lp54 molecules are packaged or at which stage of the  
423 replication cycle lp54 is packaged is unknown. In *B. burgdorferi*, both the linear  
424 chromosome and linear plasmids have covalently closed hairpin telomeres and replicate  
425 via a telomere resolution mechanism [53, 55, 86, 87]. Examination of a naturally occurring

426 Ip54 dimer in *B. valaisiana* isolate VS116 suggests that a circular head-to-head dimer is  
427 produced during Ip54 replication prior to telomere resolution and replication completion  
428 [88]. Linear, covalently closed Ip54 molecules may be packaged or Ip54 replication  
429 intermediates may be packaged.

430 As obligate vector-borne bacteria, Lyme disease spirochetes live relatively  
431 restrictive lifestyles that might be expected to i) limit their exposure to novel gene pools,  
432 ii) enhance reductive evolution, and iii) favor the loss of mobile DNA elements. A role for  
433  $\phi$ BB-1 in mediating the transduction of beneficial alleles between heterologous  
434 spirochetes in local vector and reservoir host populations may explain why cp32  
435 prophages are ubiquitous not only among Lyme disease spirochetes, but also relapsing  
436 fever spirochetes.

437 **Acknowledgments**

438 We are grateful to Patti Rosa for helpful discussions and to the IDeA National  
439 Resource for Quantitative Proteomics Center at the University of Arkansas for their  
440 assistance with proteomic analyses of phage virions. PRS is supported by NIH grants  
441 R21AI151597 and P30GM140963 (PRS). DRF is supported by NSF GRFP grant 366502.  
442 A.S-F. is a M. Jane Williams and Valerie Vargo Presidential Assistant Professor of Biology  
443 and is supported by the National Institutes of Health (K99GM147842, R00GM147842),  
444 and by the Postdoctoral Enrichment Program Award from the Burroughs Wellcome Fund  
445 (G-1021106.01). The funders had no role in study design, data collection and analysis,  
446 decision to publish, or preparation of the manuscript. The authors declare no conflicts of  
447 interest.

448 **Methods**

449 **ϕBB-1 induction.** *Borrelia burgdorferi* B31 or CA-11.2A was grown in BSK-II growth  
450 medium to  $7 \times 10^7$ /mL, transferred to 50 mL tubes and centrifuged at  $6,000 \times g$ , 10 min,  
451 35°C. Supernatants were discarded and the pellet resuspended in fresh media to a  
452 density of  $2 \times 10^8$  cells/mL. 100% EtOH was added to a final concentration of 5% (do not  
453 use 95% EtOH) and incubated at 35°C for 2 hours. The culture was centrifuged at  $6,000$   
454  $\times g$  for 10 min., 35°C. and the pellet resuspended in fresh media to a density of  $5 \times 10^7$   
455 cells/mL. The sample was incubated at 35°C for 72 hours followed by filtration through  
456 0.2  $\mu$ m filter. Samples were stored at 4°C or phage were concentrated using a 10 kDa  
457 MW cutoff filter, replacing culture medium with SM buffer.

458 **cp32 qPCR.** Packaged cp32 molecules in DNase-treated supernatants were measured  
459 by qPCR using primers that amplify a conserved cp32 intergenic region between  
460 *bbp08* and *bbp09* (5'-CTTTACACATATCAAGACCTAAC, 5'-  
461 CAAACCACCCAATTCCAATTCC). Primers that amplify the *Bb flaB* gene were used to  
462 measure *B. burgdorferi* chromosomal DNA contamination (5'-  
463 TCTTTCTCTGGTGAGGGAGCT, 5'- TCCTTCCTGTTAACACCCCTCT) [89]. Absolute  
464 cp32/ϕBB-1 copy numbers were determined using a standard curve generated with a  
465 cloned copy of the target sequence. Standard curves were performed in duplicate and  
466 ranged from  $10^{10}$  copies/well down to 1 copy/well. The lower limit of detection of the assay  
467 is 175 copies/mL with a 1  $\mu$ L input. qPCR was performed in 10  $\mu$ L reaction volumes: 5  $\mu$ L  
468 SYBR green supermix (BioRad), 1  $\mu$ L primer 1 + primer 2 at 10  $\mu$ M, 3  $\mu$ L H<sub>2</sub>O, 1  $\mu$ L sample.  
469 Thermocycling parameters were as follows: Step 1: 95° C 1 min, Step 2: 95° C 15 sec.,  
470 Step 3: 55° C 30 sec, Step 4: go to step 2, 45 times, Step 6: Melt curve from 65°C to  
471 95°C in 0.5°C increments for 5 seconds.

472 **ϕBB-1 virion purification.** Phages were precipitated using an ammonium sulfate-based  
473 protocol [90] with some modifications. Briefly, cell-free supernatants were filtered and pH  
474 adjusted to 7.5 followed by the addition of 0.5M NaCl. Phages were precipitated by adding  
475 ammonium sulfate (35% w/vol, mix until completely dissolved) and incubated at 4°C for  
476 18 hours. Samples were then centrifuged at  $3,000 \times g$  for 10 min at 4°C. The pellicle on  
477 the surface was collected and resuspended in 1 mL PBS. Where appropriate, samples  
478 were dialyzed using 10-kDa MWCO cassettes against PBS at 4°C with at least four buffer  
479 exchanges.

480 **ϕBB-1 virion proteomics.** Purified virions (200  $\mu$ g total protein) were reduced, alkylated,  
481 and purified by chloroform/methanol extraction prior to digestion with sequencing grade  
482 modified porcine trypsin (Promega). Peptides were separated on an Acquity BEH C18  
483 column (100 x 1.0 mm, Waters) using an UltiMate 3000 UHPLC system (Thermo).  
484 Peptides were eluted by a 50 min gradient from 99:1 to 60:40 buffer A:B ratio (Buffer A =  
485 0.1% formic acid, 0.5% acetonitrile. Buffer B = 0.1% formic acid, 99.9% acetonitrile).  
486 Eluted peptides were ionized by electrospray (2.4 kV) followed by mass spectrometric  
487 analysis on an Orbitrap Eclipse Tribrid mass spectrometer (Thermo) using multi-notch  
488 MS3 parameters. MS data were acquired using the FTMS analyzer over a range of 375  
489 to 1500 m/z. Up to 10 MS/MS precursors were selected for HCD activation with  
490 normalized collision energy of 65 kV, followed by acquisition of MS3 reporter ion data  
491 using the FTMS analyzer over a range of 100-500 m/z. Proteins were identified and

492 quantified using MaxQuant (Max Planck Institute) TMT MS3 reporter ion quantification  
493 with a parent ion tolerance of 2.5 ppm and a fragment ion tolerance of 0.5 Da.

494 Packaged φBB-1 DNA purification. Virions collected from 4-L cultures per replicate were  
495 purified and DNase treated as described above. 10X DNase I reaction buffer (100 mM  
496 Tris-HCl, pH 7.6, 25 mM MgCl<sub>2</sub>, 5 mM CaCl<sub>2</sub>) was added to each sample to a final  
497 concentration of 1×. DNase I was added to a final concentration of 0.1 U/1 μL sample,  
498 mixed gently, and incubated at 37°C for 18 h. EDTA was added to a final concentration  
499 of 100 mM followed by SDS to a final concentration of 0.3%. Proteinase K was added to  
500 a final concentration of 100 μg/mL and incubated at 65°C for 20 min. Samples were  
501 extracted twice with an equal volume of phenol-chloroform-isoamyl alcohol (25:24:1)  
502 followed by a single extraction with an equal volume of chloroform-isoamyl alcohol (24:1).  
503 NaCl was added to 200 mM followed by 2.5 volumes of 100% EtOH. After mixing by  
504 inverting the tubes, samples were incubated at -20°C for >30 min. DNA was pelleted by  
505 centrifugation (14,000 × g for 20 min at 4°C), pellets washed with 70% EtOH, and re-spun  
506 for 20 min, at 14,000 × g 4°C. The ethanol supernatant was discarded, and the pellet  
507 gently air-dried followed by resuspension in Tris-HCl, pH 8. Samples immediately  
508 proceeded to library preparation and sequencing.

509 Long-read sequencing library preparation. Full-length DNA molecules were ligated with  
510 multiplexing adapters and sequenced directly using the Nanopore MinION platform (FLO-  
511 MIN112 flowcell, sequencing kit SQK-LSK112 and barcoding kit SQK-NBD112.24).  
512 Quality control and adapter trimming was performed with bcl2fastq and porechop. Reads  
513 were deposited in the NCBI BioProject database accession [PRJNA1059007](#) and in  
514 Supplementary Data File 2.

515 Sequence analysis pipeline. Adapter-trimmed long-reads with quality scores ≥7 were  
516 used to isolate ≥ 5kb reads using Filtlong (v0.2.1). ≥5kb reads were mapped to the  
517 reference *B. burgdorferi* CA-11.2A genome (RefSeq assembly: GCF\_000172315.2) with  
518 minimap2 (v2.26-r1175) [91]. Primary mapping reads with MAPQ >20 were isolated by  
519 contig, filtered, and converted to final file formats using Samtools (v1.17) [92] and SeqKit  
520 (v2.5.1) [93]. Read statistics for each replicate were graphed and viewed using GraphPad  
521 Prism (v10.1.1). For each contig, *de novo* assemblies were created using Trycycler  
522 (v0.5.4) [94], which relied on input assemblies from Flye (v2.9.2-b1786) [95], Raven  
523 (v1.8.3) [96], and Minimap2/Miniasm/Minipolish (v2.26-r1175/v0.3-r179/v0.1.2) [91, 97].  
524 The long-read *de novo* assemblies were then polished with short reads using Minipolish  
525 (v0.1.2) [97]. The telomeres of the linear chromosome and linear plasmids were manually  
526 identified in SnapGene (v5.3.3), and the hairpin structures were predicted by the Mfold  
527 webserver (<http://www.unafold.org/mfold/applications/dna-folding-form.php>) [98]. The  
528 terminal ends of the cp32 prophage genomes were predicted using PhageTerm through  
529 the Galaxy webserver (<https://galaxy.pasteur.fr/>) [47], via input of the ≥5kb long-read  
530 sequences. Coverage maps of the primary mapping or primary and supplementary  
531 mapping reads were created by mapping ≥5kb long-reads to the *de novo* assembled CA-  
532 11.2A genome or the reference *B. burgdorferi* CA-11.2A genome with Minimap2,  
533 converted to final file formats using Samtools, and viewed using R (v4.3.2) and ggplot2

534 (v3.4.4).

535 Pac site cloning and qPCR. The shuttle vector pBSV2 [48] was digested with NotI to  
536 remove the promoter region and re-ligated. The *pac* region from CA-11.2A genomic DNA  
537 was amplified using primers 5'-TGGGTTGTAGAGTGGCTGTG and  
538 5'-TCACCACTTGCATAATTCTTGC and cloned into the NotI site of digested pBSV2. All  
539 vectors were sequence verified by long-read sequencing (Plasmidsaurus) and  
540 transformed into CA-11.2A. Each clone was grown in triplicate to mid-log in BSK, phage  
541 replication was induced with ethanol, virions purified, and DNase-treated as described  
542 above, followed by qPCR in triplicate using primers that target the Kan resistance gene  
543 on pBSV2 (5'-CACCGGATTTCAGTCGTCACT, 5'-GATCCTGGTATCGGTCTGCG, 120  
544 bp product).

545 Identification of conserved motifs in *B. burgdorferi* cp32 isoforms. The roughly 430  
546 nucleotides upstream of the *erp26*, *erpK*, *erpG*, *ospE* and *erpK* genes of the *B. burgdorferi*  
547 CA-11.2A cp32 isoforms cp32-1, cp32-3, cp32-5, cp32-10 and cp32-13 respectively were  
548 used as queries for a discontinuous MegaBLAST against the NCBI Nucleotide collection  
549 database. The results from these first five BLASTs were combined and sequence hits  
550 with more than 80% identity were removed with CD-HIT [99]. The resulting representative  
551 sequences were used as queries for discontinuous MegaBLAST against the NCBI  
552 Nucleotide collection (nt) database, and sequence hits with more than 80% identity were  
553 removed with CD-HIT [99], and this process was iterated twice more for a total of three  
554 MegaBLAST searches with a representative list of 80% identity query sequences. The  
555 sequence hits from the final MegaBLASTs were combined and sequences with more than  
556 95% identity were removed with CD-HIT [99], generating a list of 178 sequences. These  
557 178 sequences were used as an input dataset for the MEME webserver [49], with custom  
558 parameters of “Maximum Number of Motifs” set to “10”, and “Motif Site Distribution” set  
559 to “Any number of sites per sequence”. MEME identified motifs in 160 of the input  
560 sequences. The Position Weight Matrices (PWMs) of the 10 motifs identified by MEME  
561 were used as inputs for FIMO [100] to search for significant sequence matches (q-value  
562 < 0.001) in the *B. burgdorferi* chromosome and the *B. burgdorferi* cp32-1, cp32-3, cp32-  
563 5, cp32-10, cp32-13, cp26, lp17, lp54 plasmid DNA sequences. The cp32 isoforms had  
564 nine highly conserved sequence motifs, some motifs present in multiple copies and  
565 arranged in a conserved architecture. The cp26, lp17, lp54 and chromosome sequences  
566 did not contain this conserved architecture of nine motifs (see Supplementary Data file  
567 1). The sequence logo of each motif was generated by taking the sequence fragments  
568 that MEME used to make each PWM, and submitting these sequence fragments to the  
569 WebLogo 3.0 webserver [101]. The iterative discontinuous MegaBLAST searches had  
570 introduced eukaryotic sequence fragments into the list of 178 non-redundant sequences,  
571 suggesting that the search likely reached an endpoint and found most of the related  
572 sequences in the NCBI database. To generate a phylogenetic tree, eukaryotic sequence  
573 fragments were first removed, and the remaining 149 non-redundant sequences were  
574 aligned using the MAFFT webserver [102], with custom parameters of “Direction of  
575 nucleotide sequences” set to “Adjust direction according to the first sequence”, and  
576 “Strategy” set to E-INS-2. The resulting aligned sequence fasta file was used as input for

577 the IQ-TREE webserver [103, 104], with the following command-line: path\_to\_iqtree -s  
578 149\_aligned\_Borrelia\_\_plasmid\_sequences.fasta.fasta -st DNA -m TEST -bb 1000 -alrt  
579 1000. TreeViewer was used to display the phylogenetic tree [105].

## 580 References

- 581 1. Mead PS. Epidemiology of Lyme disease. *Infect Dis Clin North Am.* 2015;29(2):187-210. Epub 2015/05/23. doi: 10.1016/j.idc.2015.02.010. PubMed PMID: 25999219.
- 584 2. Adrion ER, Aucott J, Lemke KW, Weiner JP. Health care costs, utilization and 585 patterns of care following Lyme disease. *PLoS One.* 2015;10(2):e0116767. Epub 586 2015/02/05. doi: 10.1371/journal.pone.0116767. PubMed PMID: 25650808; PubMed 587 Central PMCID: PMC4317177.
- 588 3. Radolf JD, Strle K, Lemieux JE, Strle F. Lyme Disease in Humans. *Curr Issues 589 Mol Biol.* 2021;42:333-84. Epub 20201211. doi: 10.21775/cimb.042.333. PubMed PMID: 590 33303701; PubMed Central PMCID: PMCPMC7946767.
- 591 4. Schwartz I, Margos G, Casjens SR, Qiu WG, Eggers CH. Multipartite Genome of 592 Lyme Disease Borrelia: Structure, Variation and Prophages. *Curr Issues Mol Biol.* 593 2021;42:409-54. Epub 20201217. doi: 10.21775/cimb.042.409. PubMed PMID: 594 33328355.
- 595 5. Casjens SR, Mongodin EF, Qiu WG, Luft BJ, Schutzer SE, Gilcrease EB, et al. 596 Genome stability of Lyme disease spirochetes: comparative genomics of *Borrelia 597 burgdorferi* plasmids. *PLoS One.* 2012;7(3):e33280. Epub 20120314. doi: 598 10.1371/journal.pone.0033280. PubMed PMID: 22432010; PubMed Central PMCID: 599 PMCPMC3303823.
- 600 6. Casjens S, Palmer N, van Vugt R, Huang WM, Stevenson B, Rosa P, et al. A 601 bacterial genome in flux: the twelve linear and nine circular extrachromosomal DNAs in 602 an infectious isolate of the Lyme disease spirochete *Borrelia burgdorferi*. *Mol Microbiol.* 603 2000;35(3):490-516. Epub 2000/02/15. PubMed PMID: 10672174.
- 604 7. Samuels DS, Lybecker MC, Yang XF, Ouyang Z, Bourret TJ, Boyle WK, et al. 605 Gene Regulation and Transcriptomics. *Curr Issues Mol Biol.* 2021;42:223-66. Epub 606 20201210. doi: 10.21775/cimb.042.223. PubMed PMID: 33300497; PubMed 607 Central PMCID: PMCPMC7946783.
- 608 8. Fraser CM, Casjens S, Huang WM, Sutton GG, Clayton R, Lathigra R, et al. 609 Genomic sequence of a Lyme disease spirochaete, *Borrelia burgdorferi*. *Nature.* 610 1997;390(6660):580-6. doi: 10.1038/37551. PubMed PMID: 9403685.
- 611 9. Wachter J, Cheff B, Hillman C, Carracoi V, Dorward DW, Martens C, et al. Coupled 612 induction of prophage and virulence factors during tick transmission of the Lyme 613 disease spirochete. *Nat Commun.* 2023;14(1):198. Epub 20230113. doi: 10.1038/s41467-023- 614 35897-3. PubMed PMID: 36639656; PubMed Central PMCID: PMCPMC9839762.
- 615 10. Qiu WG, Martin CL. Evolutionary genomics of *Borrelia burgdorferi* sensu lato: 616 findings, hypotheses, and the rise of hybrids. *Infect Genet Evol.* 2014;27:576-93. Epub 617 20140403. doi: 10.1016/j.meegid.2014.03.025. PubMed PMID: 24704760; PubMed 618 Central PMCID: PMCPMC4299872.
- 619 11. Brisson D, Drecktrah D, Eggers CH, Samuels DS. Genetics of *Borrelia burgdorferi*. 620 *Annu Rev Genet.* 2012;46:515-36. Epub 2012/09/15. doi: 10.1146/annurev-genet- 621 011112-112140. PubMed PMID: 22974303; PubMed Central PMCID: 622 PMCPMC3856702.
- 623 12. Qiu WG, Bosler EM, Campbell JR, Ugine GD, Wang IN, Luft BJ, et al. A population 624 genetic study of *Borrelia burgdorferi* sensu stricto from eastern Long Island, New York,

625 suggested frequency-dependent selection, gene flow and host adaptation. *Hereditas*.  
626 1997;127(3):203-16. doi: 10.1111/j.1601-5223.1997.00203.x. PubMed PMID: 9474903.

627 13. Haven J, Vargas LC, Mongodin EF, Xue V, Hernandez Y, Pagan P, et al. Pervasive  
628 recombination and sympatric genome diversification driven by frequency-dependent  
629 selection in *Borrelia burgdorferi*, the Lyme disease bacterium. *Genetics*.  
630 2011;189(3):951-66. Epub 20110902. doi: 10.1534/genetics.111.130773. PubMed PMID:  
631 21890743; PubMed Central PMCID: PMCPMC3213364.

632 14. Combs MA, Tufts DM, Adams B, Lin YP, Kolokotronis SO, Diuk-Wasser MA. Host  
633 adaptation drives genetic diversity in a vector-borne disease system. *PNAS Nexus*.  
634 2023;2(8):pgad234. Epub 20230808. doi: 10.1093/pnasnexus/pgad234. PubMed PMID:  
635 37559749; PubMed Central PMCID: PMCPMC10408703.

636 15. Brisson D, Zhou W, Jutras BL, Casjens S, Stevenson B. Distribution of cp32  
637 prophages among Lyme disease-causing spirochetes and natural diversity of their  
638 lipoprotein-encoding *erp* loci. *Appl Environ Microbiol*. 2013;79(13):4115-28. Epub  
639 20130426. doi: 10.1128/AEM.00817-13. PubMed PMID: 23624478; PubMed Central  
640 PMCID: PMCPMC3697573.

641 16. Casjens SR, Gilcrease EB, Vujadinovic M, Mongodin EF, Luft BJ, Schutzer SE, et  
642 al. Plasmid diversity and phylogenetic consistency in the Lyme disease agent *Borrelia*  
643 *burgdorferi*. *BMC Genomics*. 2017;18(1):165. Epub 20170215. doi: 10.1186/s12864-017-  
644 3553-5. PubMed PMID: 28201991; PubMed Central PMCID: PMCPMC5310021.

645 17. Margos G, Hepner S, Mang C, Marosevic D, Reynolds SE, Krebs S, et al. Lost in  
646 plasmids: next generation sequencing and the complex genome of the tick-borne  
647 pathogen *Borrelia burgdorferi*. *BMC Genomics*. 2017;18(1):422. Epub 2017/06/01. doi:  
648 10.1186/s12864-017-3804-5. PubMed PMID: 28558786; PubMed Central PMCID:  
649 PMCPMC5450258.

650 18. Touchon M, Moura de Sousa JA, Rocha EP. Embracing the enemy: the  
651 diversification of microbial gene repertoires by phage-mediated horizontal gene transfer.  
652 *Curr Opin Microbiol*. 2017;38:66-73. Epub 20170517. doi: 10.1016/j.mib.2017.04.010.  
653 PubMed PMID: 28527384.

654 19. Brissette CA, Haupt K, Barthel D, Cooley AE, Bowman A, Skerka C, et al. *Borrelia*  
655 *burgdorferi* infection-associated surface proteins *ErpP*, *ErpA*, and *ErpC* bind human  
656 plasminogen. *Infect Immun*. 2009;77(1):300-6. Epub 2008/11/13. doi: 10.1128/IAI.01133-  
657 08. PubMed PMID: 19001079; PubMed Central PMCID: PMCPMC2612283.

658 20. Brissette CA, Cooley AE, Burns LH, Riley SP, Verma A, Woodman ME, et al. Lyme  
659 borreliosis spirochete *Erp* proteins, their known host ligands, and potential roles in  
660 mammalian infection. *Int J Med Microbiol*. 2008;298 Suppl 1:257-67. Epub 20080111.  
661 doi: 10.1016/j.ijmm.2007.09.004. PubMed PMID: 18248770; PubMed Central PMCID:  
662 PMCPMC2596196.

663 21. Stevenson B, Bono JL, Schwan TG, Rosa P. *Borrelia burgdorferi* *erp* proteins are  
664 immunogenic in mammals infected by tick bite, and their synthesis is inducible in cultured  
665 bacteria. *Infect Immun*. 1998;66(6):2648-54. Epub 1998/05/29. doi:  
666 10.1128/IAI.66.6.2648-2654.1998. PubMed PMID: 9596729; PubMed Central PMCID:  
667 PMCPMC108251.

668 22. Stevenson B, Zuckert WR, Akins DR. Repetition, conservation, and variation: the  
669 multiple cp32 plasmids of *Borrelia* species. *J Mol Microbiol Biotechnol*. 2000;2(4):411-22.  
670 Epub 2000/11/15. PubMed PMID: 11075913.

671 23. Kenedy MR, Lenhart TR, Akins DR. The role of *Borrelia burgdorferi* outer surface  
672 proteins. *FEMS Immunol Med Microbiol*. 2012;66(1):1-19. Epub 20120521. doi:  
673 10.1111/j.1574-695X.2012.00980.x. PubMed PMID: 22540535; PubMed Central PMCID:  
674 PMCPMC3424381.

675 24. Stevenson B, Casjens S, Rosa P. Evidence of past recombination events among  
676 the genes encoding the Erp antigens of *Borrelia burgdorferi*. *Microbiology (Reading)*.  
677 1998;144 ( Pt 7):1869-79. doi: 10.1099/00221287-144-7-1869. PubMed PMID: 9695920.

678 25. Stevenson B, Miller JC. Intra- and interbacterial genetic exchange of Lyme disease  
679 spirochete erp genes generates sequence identity amidst diversity. *J Mol Evol*.  
680 2003;57(3):309-24. Epub 2003/11/25. doi: 10.1007/s00239-003-2482-x. PubMed PMID:  
681 14629041.

682 26. Qiu WG, Schutzer SE, Bruno JF, Attie O, Xu Y, Dunn JJ, et al. Genetic exchange  
683 and plasmid transfers in *Borrelia burgdorferi* sensu stricto revealed by three-way genome  
684 comparisons and multilocus sequence typing. *Proc Natl Acad Sci U S A*.  
685 2004;101(39):14150-5. Epub 2004/09/16. doi: 10.1073/pnas.0402745101. PubMed PMID:  
686 15375210; PubMed Central PMCID: PMCPMC521097.

687 27. Sapiro AL, Hayes BM, Volk RF, Zhang JY, Brooks DM, Martyn C, et al. Longitudinal map of transcriptome changes in the Lyme pathogen *Borrelia burgdorferi*  
688 during tick-borne transmission. *Elife*. 2023;12. Epub 2023/07/14. doi: 10.7554/eLife.86636.  
689 PubMed PMID: 37449477.

690 28. Tokarz R, Anderton JM, Katona LI, Benach JL. Combined effects of blood and  
691 temperature shift on *Borrelia burgdorferi* gene expression as determined by whole  
692 genome DNA array. *Infect Immun*. 2004;72(9):5419-32. doi: 10.1128/IAI.72.9.5419-  
693 5432.2004. PubMed PMID: 15322040; PubMed Central PMCID: PMCPMC517457.

694 29. Eggers CH, Kimmel BJ, Bono JL, Elias AF, Rosa P, Samuels DS. Transduction by  
695 phiBB-1, a bacteriophage of *Borrelia burgdorferi*. *J Bacteriol*. 2001;183(16):4771-8. doi:  
696 10.1128/JB.183.16.4771-4778.2001. PubMed PMID: 11466280; PubMed Central  
697 PMCID: PMCPMC99531.

698 30. Eggers CH, Samuels DS. Molecular evidence for a new bacteriophage of *Borrelia*  
699 *burgdorferi*. *J Bacteriol*. 1999;181(23):7308-13. Epub 1999/11/26. PubMed PMID:  
700 10572135; PubMed Central PMCID: PMCPMC103694.

701 31. Zhang H, Marconi RT. Demonstration of cotranscription and 1-methyl-3-nitroso-  
702 nitroguanidine induction of a 30-gene operon of *Borrelia burgdorferi*: evidence that the  
703 32-kilobase circular plasmids are prophages. *J Bacteriol*. 2005;187(23):7985-95. Epub  
704 2005/11/18. doi: 10.1128/JB.187.23.7985-7995.2005. PubMed PMID: 16291672;  
705 PubMed Central PMCID: PMCPMC1291276.

706 32. Fillol-Salom A, Alsaadi A, Sousa JAM, Zhong L, Foster KR, Rocha EPC, et al.  
707 Bacteriophages benefit from generalized transduction. *PLoS Pathog*.  
708 2019;15(7):e1007888. Epub 2019/07/06. doi: 10.1371/journal.ppat.1007888. PubMed  
709 PMID: 31276485; PubMed Central PMCID: PMCPMC6636781.

710 33. Zinder ND, Lederberg J. Genetic exchange in *Salmonella*. *J Bacteriol*.  
711 1952;64(5):679-99. doi: 10.1128/jb.64.5.679-699.1952. PubMed PMID: 12999698;  
712 PubMed Central PMCID: PMCPMC169409.

713 34. Budzik JM, Rosche WA, Rietsch A, O'Toole GA. Isolation and characterization of  
714 a generalized transducing phage for *Pseudomonas aeruginosa* strains PAO1 and PA14.  
715 *J Bacteriol*. 2004;186(10):3270-3. Epub 2004/05/06. doi: 10.1128/JB.186.10.3270-  
716 3273.2004. PubMed PMID: 15126493; PubMed Central PMCID: PMCPMC400619.

717 35. Mandecki W, Krajewska-Grynkiewicz K, Klopotowski T. A quantitative model for  
718 nonrandom generalized transduction, applied to the phage P22-*Salmonella typhimurium*  
719 system. *Genetics*. 1986;114(2):633-57. Epub 1986/10/01. PubMed PMID: 3021574;  
720 PubMed Central PMCID: PMCPMC1202961.

721 36. Ebel-Tsipis J, Botstein D, Fox MS. Generalized transduction by phage P22 in  
722 *Salmonella typhimurium*. I. Molecular origin of transducing DNA. *J Mol Biol*.  
723

724 1972;71(2):433-48. Epub 1972/11/14. doi: 10.1016/0022-2836(72)90361-0. PubMed  
725 PMID: 4564486.

726 37. Chiang YN, Penades JR, Chen J. Genetic transduction by phages and  
727 chromosomal islands: The new and noncanonical. PLoS Pathog. 2019;15(8):e1007878.  
728 Epub 20190808. doi: 10.1371/journal.ppat.1007878. PubMed PMID: 31393945; PubMed  
729 Central PMCID: PMCPMC6687093.

730 38. Eggers CH, Gray CM, Preisig AM, Glenn DM, Pereira J, Ayers RW, et al. Phage-  
731 mediated horizontal gene transfer of both prophage and heterologous DNA by varphiBB-  
732 1, a bacteriophage of *Borrelia burgdorferi*. Pathog Dis. 2016;74(9). Epub 2016/11/05. doi:  
733 10.1093/femspd/ftw107. PubMed PMID: 27811049.

734 39. Eggers CH. Identification and characterization of a bacteriophage of *Borrelia*  
735 *burgdorferi* Graduate Student Theses, Dissertations, & Professional Papers 10590. 2000.

736 40. Rumnieks J, Fuzik T, Tars K. Structure of the *Borrelia* bacteriophage phiBB1  
737 procapsid. J Mol Biol. 2023;168323. Epub 20231020. doi: 10.1016/j.jmb.2023.168323.  
738 PubMed PMID: 37866476.

739 41. Eggers CH, Casjens S, Hayes SF, Garon CF, Damman CJ, Oliver DB, et al.  
740 Bacteriophages of spirochetes. J Mol Microbiol Biotechnol. 2000;2(4):365-73. Epub  
741 2000/11/15. PubMed PMID: 11075907.

742 42. Neubert U, Schaller M, Januschke E, Stoltz W, Schmieger H. Bacteriophages  
743 induced by ciprofloxacin in a *Borrelia burgdorferi* skin isolate. Zentralbl Bakteriol.  
744 1993;279(3):307-15. doi: 10.1016/s0934-8840(11)80363-4. PubMed PMID: 8219501.

745 43. Gillis M, De Ley J, De Cleene M. The determination of molecular weight of bacterial  
746 genome DNA from renaturation rates. Eur J Biochem. 1970;12(1):143-53. doi:  
747 10.1111/j.1432-1033.1970.tb00831.x. PubMed PMID: 4984994.

748 44. Wood DE, Salzberg SL. Kraken: ultrafast metagenomic sequence classification  
749 using exact alignments. Genome Biol. 2014;15(3):R46. Epub 20140303. doi: 10.1186/gb-  
750 2014-15-3-r46. PubMed PMID: 24580807; PubMed Central PMCID: PMCPMC4053813.

751 45. Schutzer SE, Fraser-Liggett CM, Casjens SR, Qiu WG, Dunn JJ, Mongodin EF, et  
752 al. Whole-genome sequences of thirteen isolates of *Borrelia burgdorferi*. J Bacteriol.  
753 2011;193(4):1018-20. Epub 20101008. doi: 10.1128/JB.01158-10. PubMed PMID:  
754 20935092; PubMed Central PMCID: PMCPMC3028687.

755 46. Casjens SR, Gilcrease EB. Determining DNA packaging strategy by analysis of  
756 the termini of the chromosomes in tailed-bacteriophage virions. Methods Mol Biol.  
757 2009;502:91-111. doi: 10.1007/978-1-60327-565-1\_7. PubMed PMID: 19082553;  
758 PubMed Central PMCID: PMCPMC3082370.

759 47. Garneau JR, Depardieu F, Fortier LC, Bikard D, Monot M. PhageTerm: a tool for  
760 fast and accurate determination of phage termini and packaging mechanism using next-  
761 generation sequencing data. Sci Rep. 2017;7(1):8292. Epub 20170815. doi:  
762 10.1038/s41598-017-07910-5. PubMed PMID: 28811656; PubMed Central PMCID:  
763 PMCPMC5557969.

764 48. Stewart PE, Thalken R, Bono JL, Rosa P. Isolation of a circular plasmid region  
765 sufficient for autonomous replication and transformation of infectious *Borrelia burgdorferi*.  
766 Mol Microbiol. 2001;39(3):714-21. doi: 10.1046/j.1365-2958.2001.02256.x. PubMed  
767 PMID: 11169111.

768 49. Bailey TL, Boden M, Buske FA, Frith M, Grant CE, Clementi L, et al. MEME SUITE:  
769 tools for motif discovery and searching. Nucleic Acids Res. 2009;37(Web Server  
770 issue):W202-8. Epub 20090520. doi: 10.1093/nar/gkp335. PubMed PMID: 19458158;  
771 PubMed Central PMCID: PMCPMC2703892.

772 50. Casjens S. Evolution of the linear DNA replicons of the *Borrelia* spirochetes. *Curr*  
773 *Opin Microbiol.* 1999;2(5):529-34. doi: 10.1016/s1369-5274(99)00012-0. PubMed PMID:  
774 10508719.

775 51. Tourand Y, Bankhead T, Wilson SL, Putteet-Driver AD, Barbour AG, Byram R, et  
776 al. Differential telomere processing by *Borrelia* telomere resolvases in vitro but not in vivo.  
777 *J Bacteriol.* 2006;188(21):7378-86. Epub 20060825. doi: 10.1128/JB.00760-06. PubMed  
778 PMID: 16936037; PubMed Central PMCID: PMCPMC1636258.

779 52. Tourand Y, Kobryn K, Chaconas G. Sequence-specific recognition but position-  
780 dependent cleavage of two distinct telomeres by the *Borrelia burgdorferi* telomere  
781 resolvase, ResT. *Mol Microbiol.* 2003;48(4):901-11. doi: 10.1046/j.1365-  
782 2958.2003.03485.x. PubMed PMID: 12753185.

783 53. Kobryn K, Chaconas G. Hairpin Telomere Resolvases. *Microbiol Spectr.*  
784 2014;2(6). doi: 10.1128/microbiolspec.MDNA3-0023-2014. PubMed PMID: 26104454.

785 54. Huang WM, Robertson M, Aron J, Casjens S. Telomere exchange between linear  
786 replicons of *Borrelia burgdorferi*. *J Bacteriol.* 2004;186(13):4134-41. doi:  
787 10.1128/JB.186.13.4134-4141.2004. PubMed PMID: 15205414; PubMed Central  
788 PMCID: PMCPMC421586.

789 55. Chaconas G, Stewart PE, Tilly K, Bono JL, Rosa P. Telomere resolution in the  
790 Lyme disease spirochete. *Embo J.* 2001;20(12):3229-37. doi:  
791 10.1093/emboj/20.12.3229. PubMed PMID: 11406599; PubMed Central PMCID:  
792 PMCPMC150187.

793 56. Casjens S, Murphy M, DeLange M, Sampson L, van Vugt R, Huang WM.  
794 Telomeres of the linear chromosomes of Lyme disease spirochaetes: nucleotide  
795 sequence and possible exchange with linear plasmid telomeres. *Mol Microbiol.*  
796 1997;26(3):581-96. doi: 10.1046/j.1365-2958.1997.6051963.x. PubMed PMID: 9402027.

797 57. Tourand Y, Deneke J, Moriarty TJ, Chaconas G. Characterization and in vitro  
798 reaction properties of 19 unique hairpin telomeres from the linear plasmids of the lyme  
799 disease spirochete. *J Biol Chem.* 2009;284(11):7264-72. Epub 20090102. doi:  
800 10.1074/jbc.M808918200. PubMed PMID: 19122193; PubMed Central PMCID:  
801 PMCPMC2652300.

802 58. Wilske B, Preac-Mursic V, Jauris S, Hofmann A, Pradel I, Soutschek E, et al.  
803 Immunological and molecular polymorphisms of OspC, an immunodominant major outer  
804 surface protein of *Borrelia burgdorferi*. *Infect Immun.* 1993;61(5):2182-91. doi:  
805 10.1128/iai.61.5.2182-2191.1993. PubMed PMID: 8478108; PubMed Central PMCID:  
806 PMCPMC280819.

807 59. Probert WS, Crawford M, Cadiz RB, LeFebvre RB. Immunization with outer  
808 surface protein (Osp) A, but not OspC, provides cross-protection of mice challenged with  
809 North American isolates of *Borrelia burgdorferi*. *J Infect Dis.* 1997;175(2):400-5. doi:  
810 10.1093/infdis/175.2.400. PubMed PMID: 9203661.

811 60. Barthold SW. Specificity of infection-induced immunity among *Borrelia burgdorferi*  
812 sensu lato species. *Infect Immun.* 1999;67(1):36-42. doi: 10.1128/IAI.67.1.36-42.1999.  
813 PubMed PMID: 9864193; PubMed Central PMCID: PMCPMC96274.

814 61. Brisson D, Vandermause MF, Meece JK, Reed KD, Dykhuizen DE. Evolution of  
815 northeastern and midwestern *Borrelia burgdorferi*, United States. *Emerg Infect Dis.*  
816 2010;16(6):911-7. doi: 10.3201/eid1606.090329. PubMed PMID: 20507740; PubMed  
817 Central PMCID: PMCPMC3086229.

818 62. Nadelman RB, Hanincova K, Mukherjee P, Liveris D, Nowakowski J, McKenna D,  
819 et al. Differentiation of reinfection from relapse in recurrent Lyme disease. *N Engl J Med.*  
820 2012;367(20):1883-90. doi: 10.1056/NEJMoa1114362. PubMed PMID: 23150958;  
821 PubMed Central PMCID: PMCPMC3526003.

822 63. Bhatia B, Hillman C, Carraco V, Cheff BN, Tilly K, Rosa PA. Infection history of  
823 the blood-meal host dictates pathogenic potential of the Lyme disease spirochete within  
824 the feeding tick vector. *PLoS Pathog.* 2018;14(4):e1006959. Epub 20180405. doi:  
825 10.1371/journal.ppat.1006959. PubMed PMID: 29621350; PubMed Central PMCID:  
826 PMCPMC5886588.

827 64. Kurtti TJ, Munderloh UG, Hughes CA, Engstrom SM, Johnson RC. Resistance to  
828 tick-borne spirochete challenge induced by *Borrelia burgdorferi* strains that differ in  
829 expression of outer surface proteins. *Infect Immun.* 1996;64(10):4148-53. doi:  
830 10.1128/iai.64.10.4148-4153.1996. PubMed PMID: 8926082; PubMed Central PMCID:  
831 PMCPMC174350.

832 65. Piesman J, Dolan MC, Happ CM, Luft BJ, Rooney SE, Mather TN, et al. Duration  
833 of immunity to reinfection with tick-transmitted *Borrelia burgdorferi* in naturally infected  
834 mice. *Infect Immun.* 1997;65(10):4043-7. doi: 10.1128/iai.65.10.4043-4047.1997.  
835 PubMed PMID: 9317005; PubMed Central PMCID: PMCPMC175581.

836 66. Hofmeister EK, Glass GE, Childs JE, Persing DH. Population dynamics of a  
837 naturally occurring heterogeneous mixture of *Borrelia burgdorferi* clones. *Infect Immun.*  
838 1999;67(11):5709-16. doi: 10.1128/IAI.67.11.5709-5716.1999. PubMed PMID:  
839 10531219; PubMed Central PMCID: PMCPMC96945.

840 67. Shang ES, Wu XY, Lovett MA, Miller JN, Blanco DR. Homologous and  
841 heterologous *Borrelia burgdorferi* challenge of infection-derived immune rabbits using  
842 host-adapted organisms. *Infect Immun.* 2001;69(1):593-8. doi: 10.1128/IAI.69.1.593-  
843 598.2001. PubMed PMID: 11119560; PubMed Central PMCID: PMCPMC97926.

844 68. Derdakova M, Dudioak V, Brei B, Brownstein JS, Schwartz I, Fish D. Interaction  
845 and transmission of two *Borrelia burgdorferi* sensu stricto strains in a tick-rodent  
846 maintenance system. *Appl Environ Microbiol.* 2004;70(11):6783-8. doi:  
847 10.1128/AEM.70.11.6783-6788.2004. PubMed PMID: 15528545; PubMed Central  
848 PMCID: PMCPMC525125.

849 69. Khatchikian CE, Nadelman RB, Nowakowski J, Schwartz I, Wormser GP, Brisson  
850 D. Evidence for strain-specific immunity in patients treated for early lyme disease. *Infect*  
851 *Immun.* 2014;82(4):1408-13. Epub 20140113. doi: 10.1128/IAI.01451-13. PubMed PMID:  
852 24421042; PubMed Central PMCID: PMCPMC3993397.

853 70. Dykhuizen DE, Polin DS, Dunn JJ, Wilske B, Preac-Mursic V, Dattwyler RJ, et al.  
854 *Borrelia burgdorferi* is clonal: implications for taxonomy and vaccine development. *Proc*  
855 *Natl Acad Sci U S A.* 1993;90(21):10163-7. doi: 10.1073/pnas.90.21.10163. PubMed  
856 PMID: 8234271; PubMed Central PMCID: PMCPMC47734.

857 71. Marconi RT, Samuels DS, Landry RK, Garon CF. Analysis of the distribution and  
858 molecular heterogeneity of the *ospD* gene among the Lyme disease spirochetes:  
859 evidence for lateral gene exchange. *J Bacteriol.* 1994;176(15):4572-82. doi:  
860 10.1128/jb.176.15.4572-4582.1994. PubMed PMID: 7913928; PubMed Central PMCID:  
861 PMCPMC196277.

862 72. Stevenson B, Barthold SW. Expression and sequence of outer surface protein C  
863 among North American isolates of *Borrelia burgdorferi*. *FEMS Microbiol Lett.*  
864 1994;124(3):367-72. doi: 10.1111/j.1574-6968.1994.tb07310.x. PubMed PMID:  
865 7851744.

866 73. Jauris-Heipke S, Liegl G, Preac-Mursic V, Rossler D, Schwab E, Soutschek E, et  
867 al. Molecular analysis of genes encoding outer surface protein C (OspC) of *Borrelia*  
868 *burgdorferi* sensu lato: relationship to *ospA* genotype and evidence of lateral gene  
869 exchange of *ospC*. *J Clin Microbiol.* 1995;33(7):1860-6. doi: 10.1128/jcm.33.7.1860-  
870 1866.1995. PubMed PMID: 7665660; PubMed Central PMCID: PMCPMC228286.

871 74. Livey I, Gibbs CP, Schuster R, Dorner F. Evidence for lateral transfer and  
872 recombination in OspC variation in Lyme disease Borrelia. *Mol Microbiol*. 1995;18(2):257-  
873 69. doi: 10.1111/j.1365-2958.1995.mmi\_18020257.x. PubMed PMID: 8709845.

874 75. Will G, Jauris-Heipke S, Schwab E, Busch U, Rossler D, Soutschek E, et al. Sequence analysis of ospA genes shows homogeneity within *Borrelia burgdorferi* sensu stricto and *Borrelia afzelii* strains but reveals major subgroups within the *Borrelia garinii* species. *Med Microbiol Immunol*. 1995;184(2):73-80. doi: 10.1007/BF00221390. PubMed PMID: 7500914.

879 76. Hefty PS, Brooks CS, Jett AM, White GL, Wikle SK, Kennedy RC, et al. OspE-related, OspF-related, and Elp lipoproteins are immunogenic in baboons experimentally infected with *Borrelia burgdorferi* and in human lyme disease patients. *J Clin Microbiol*. 2002;40(11):4256-65. Epub 2002/11/01. PubMed PMID: 12409407; PubMed Central PMCID: PMCPMC139709.

884 77. Tilly K, Bestor A, Rosa PA. Functional Equivalence of OspA and OspB, but Not OspC, in Tick Colonization by *Borrelia burgdorferi*. *Infect Immun*. 2016;84(5):1565-73. Epub 20160422. doi: 10.1128/IAI.00063-16. PubMed PMID: 26953324; PubMed Central PMCID: PMCPMC4862709.

888 78. Battisti JM, Bono JL, Rosa PA, Schrumpf ME, Schwan TG, Policastro PF. Outer surface protein A protects Lyme disease spirochetes from acquired host immunity in the tick vector. *Infect Immun*. 2008;76(11):5228-37. Epub 20080908. doi: 10.1128/IAI.00410-08. PubMed PMID: 18779341; PubMed Central PMCID: PMCPMC2573341.

892 79. Yang XF, Pal U, Alani SM, Fikrig E, Norgard MV. Essential role for OspA/B in the life cycle of the Lyme disease spirochete. *J Exp Med*. 2004;199(5):641-8. Epub 20040223. doi: 10.1084/jem.20031960. PubMed PMID: 14981112; PubMed Central PMCID: PMCPMC2213294.

896 80. Wang IN, Dykhuizen DE, Qiu W, Dunn JJ, Bosler EM, Luft BJ. Genetic diversity of ospC in a local population of *Borrelia burgdorferi* sensu stricto. *Genetics*. 1999;151(1):15-30. doi: 10.1093/genetics/151.1.15. PubMed PMID: 9872945; PubMed Central PMCID: PMCPMC1460459.

900 81. Lemieux JE, Huang W, Hill N, Cerar T, Freimark L, Hernandez S, et al. Whole genome sequencing of human *Borrelia burgdorferi* isolates reveals linked blocks of accessory genome elements located on plasmids and associated with human dissemination. *PLoS Pathog*. 2023;19(8):e1011243. Epub 20230831. doi: 10.1371/journal.ppat.1011243. PubMed PMID: 37651316; PubMed Central PMCID: PMCPMC10470944.

906 82. Streisinger G, Emrich J, Stahl MM. Chromosome structure in phage t4, iii. Terminal redundancy and length determination. *Proc Natl Acad Sci U S A*. 1967;57(2):292-5. doi: 10.1073/pnas.57.2.292. PubMed PMID: 16591467; PubMed Central PMCID: PMCPMC335503.

910 83. Beaulaurier J, Luo E, Eppley JM, Uyl PD, Dai X, Burger A, et al. Assembly-free single-molecule sequencing recovers complete virus genomes from natural microbial communities. *Genome Res*. 2020;30(3):437-46. Epub 2020/02/23. doi: 10.1101/gr.251686.119. PubMed PMID: 32075851; PubMed Central PMCID: PMCPMC7111524.

915 84. Skare JT, Champion CI, Mirzabekov TA, Shang ES, Blanco DR, Erdjument-Bromage H, et al. Porin activity of the native and recombinant outer membrane protein Oms28 of *Borrelia burgdorferi*. *J Bacteriol*. 1996;178(16):4909-18. doi: 10.1128/jb.178.16.4909-4918.1996. PubMed PMID: 8759855; PubMed Central PMCID: PMCPMC178274.

920 85. Kasumba IN, Tilly K, Lin T, Norris SJ, Rosa PA. Strict Conservation yet Non-  
921 Essential Nature of Plasmid Gene *bba40* in the Lyme Disease Spirochete *Borrelia*  
922 *burgdorferi*. *Microbiol Spectr*. 2023;11(3):e0047723. Epub 20230403. doi:  
923 10.1128/spectrum.00477-23. PubMed PMID: 37010416; PubMed Central PMCID:  
924 PMCPMC10269632.

925 86. Barbour AG, Garon CF. Linear plasmids of the bacterium *Borrelia burgdorferi* have  
926 covalently closed ends. *Science*. 1987;237(4813):409-11. doi: 10.1126/science.3603026.  
927 PubMed PMID: 3603026.

928 87. Hinnebusch J, Tilly K. Linear plasmids and chromosomes in bacteria. *Mol*  
929 *Microbiol*. 1993;10(5):917-22. doi: 10.1111/j.1365-2958.1993.tb00963.x. PubMed PMID:  
930 7934868.

931 88. Marconi RT, Casjens S, Munderloh UG, Samuels DS. Analysis of linear plasmid  
932 dimers in *Borrelia burgdorferi* sensu lato isolates: implications concerning the potential  
933 mechanism of linear plasmid replication. *J Bacteriol*. 1996;178(11):3357-61. doi:  
934 10.1128/jb.178.11.3357-3361.1996. PubMed PMID: 8655522; PubMed Central PMCID:  
935 PMCPMC178094.

936 89. Pahl A, Kuhlbrandt U, Brune K, Rollinghoff M, Gessner A. Quantitative detection  
937 of *Borrelia burgdorferi* by real-time PCR. *J Clin Microbiol*. 1999;37(6):1958-63. doi:  
938 10.1128/JCM.37.6.1958-1963.1999. PubMed PMID: 10325354; PubMed Central PMCID:  
939 PMCPMC84995.

940 90. Armon R, Arella M, Payment P. A highly efficient second-step concentration  
941 technique for bacteriophages and enteric viruses using ammonium sulfate and Tween 80.  
942 *Can J Microbiol*. 1988;34(5):651-5. doi: 10.1139/m88-107. PubMed PMID: 2850100.

943 91. Li H. Minimap2: pairwise alignment for nucleotide sequences. *Bioinformatics*.  
944 2018;34(18):3094-100. doi: 10.1093/bioinformatics/bty191.

945 92. Danecek P, Bonfield JK, Liddle J, Marshall J, Ohan V, Pollard MO, et al. Twelve  
946 years of SAMtools and BCFtools. *GigaScience*. 2021;10(2). doi:  
947 10.1093/gigascience/giab008.

948 93. Shen W, Le S, Li Y, Hu F. SeqKit: A Cross-Platform and Ultrafast Toolkit for  
949 FASTA/Q File Manipulation. *PLOS ONE*. 2016;11(10):e0163962. doi:  
950 10.1371/journal.pone.0163962.

951 94. Wick RR, Judd LM, Cerdeira LT, Hawkey J, Méric G, Vezina B, et al. Trycycler:  
952 consensus long-read assemblies for bacterial genomes. *Genome Biology*. 2021;22(1).  
953 doi: 10.1186/s13059-021-02483-z.

954 95. Kolmogorov M, Yuan J, Lin Y, Pevzner PA. Assembly of long, error-prone reads  
955 using repeat graphs. *Nature Biotechnology*. 2019;37(5):540-6. doi: 10.1038/s41587-019-  
956 0072-8.

957 96. Vaser R, Šikić M. Time- and memory-efficient genome assembly with Raven.  
958 *Nature Computational Science*. 2021;1(5):332-6. doi: 10.1038/s43588-021-00073-4.

959 97. Wick RR, Holt KE. Benchmarking of long-read assemblers for prokaryote whole  
960 genome sequencing. *F1000Research*. 2021;8:2138. doi:  
961 10.12688/f1000research.21782.4.

962 98. Zuker M. Mfold web server for nucleic acid folding and hybridization prediction.  
963 *Nucleic Acids Research*. 2003;31(13):3406-15. doi: 10.1093/nar/gkg595.

964 99. Fu L, Niu B, Zhu Z, Wu S, Li W. CD-HIT: accelerated for clustering the next-  
965 generation sequencing data. *Bioinformatics*. 2012;28(23):3150-2. Epub 20121011. doi:  
966 10.1093/bioinformatics/bts565. PubMed PMID: 23060610; PubMed Central PMCID:  
967 PMCPMC3516142.

968 100. Grant CE, Bailey TL, Noble WS. FIMO: scanning for occurrences of a given motif.  
969 Bioinformatics. 2011;27(7):1017-8. Epub 20110216. doi: 10.1093/bioinformatics/btr064.  
970 PubMed PMID: 21330290; PubMed Central PMCID: PMCPMC3065696.

971 101. Crooks GE, Hon G, Chandonia JM, Brenner SE. WebLogo: a sequence logo  
972 generator. Genome Res. 2004;14(6):1188-90. Epub 2004/06/03. doi: 10.1101/gr.849004.  
973 PubMed PMID: 15173120; PubMed Central PMCID: PMCPMC419797.

974 102. Katoh K, Standley DM. MAFFT multiple sequence alignment software version 7:  
975 improvements in performance and usability. Mol Biol Evol. 2013;30(4):772-80. Epub  
976 20130116. doi: 10.1093/molbev/mst010. PubMed PMID: 23329690; PubMed Central  
977 PMCID: PMCPMC3603318.

978 103. Nguyen LT, Schmidt HA, von Haeseler A, Minh BQ. IQ-TREE: a fast and effective  
979 stochastic algorithm for estimating maximum-likelihood phylogenies. Mol Biol Evol.  
980 2015;32(1):268-74. Epub 20141103. doi: 10.1093/molbev/msu300. PubMed PMID:  
981 25371430; PubMed Central PMCID: PMCPMC4271533.

982 104. Minh BQ, Nguyen MA, von Haeseler A. Ultrafast approximation for phylogenetic  
983 bootstrap. Mol Biol Evol. 2013;30(5):1188-95. Epub 20130215. doi:  
984 10.1093/molbev/mst024. PubMed PMID: 23418397; PubMed Central PMCID:  
985 PMCPMC3670741.

986 105. Bianchini G, Sánchez-Baracaldo P. TreeViewer - Cross-platform software to draw  
987 phylogenetic trees. 2023. doi: <https://doi.org/10.5281/zenodo.7768343>.

988